NATIVE CHEMICAL LIGATION DIRECTED PEPTIDE SELF ASSEMBLY

M.Sc. Thesis

By SHREYASHI SARKAR



DEPARTMENT OF CHEMISTRY INDIAN INSTITUTE OF TECHNOLOGY INDORE

MAY, 2025

NATIVE CHEMICAL LIGATION DIRECTED PEPTIDE SELF ASSEMBLY

A THESIS

Submitted in partial fulfillment of the requirements for the award of the degree

of

Master of Science

by

SHREYASHI SARKAR



DEPARTMENT OF CHEMISTRY INDIAN INSTITUTE OF TECHNOLOGY INDORE MAY 2025



INDIAN INSTITUTE OF TECHNOLOGY INDORE

DECLARATION

I hereby certify that the work which is being presented in the thesis entitled "Native Chemical Ligation Directed Peptide Self Assembly" in the partial fulfillment of the requirements for the award of the degree of MASTER OF SCIENCE and submitted in the DEPARTMENT OF CHEMISTRY, Indian Institute of Technology Indore, is an authentic record of my own work carried out during the time period from July, 2024 to May, 2025 under the supervision of Prof. Apurba K Das. The matter presented in this thesis has not been submitted by me for the award of any other degree of this or any other institute.

Signature of the student with date (Shreyashi Sarkar)

This is to certify that the above statement made by the candidate is correct to the best of my/our knowledge.

ature of the Supervisor of M.Sc. thesis

(Prof. Apurba K Das)

Shreyashi Sarkar has successfully given her M.Sc. Oral Examination held on May 16, 2025.

Signature of Supervisor of MSc thesis

Date: 20/05/25

ACKNOWLEDGEMENTS

Any achievement is not an effort of a single person but it takes advice, assistance, suggestions, and inspiration from a lot of people. It's my pleasure to have their names in my thesis. I would like to express my gratitude, regard, and acknowledgment to them.

I would like to express my heartfelt gratitude to my thesis supervisor, Prof. Apurba K. Das, for his invaluable guidance, support, and encouragement throughout my research journey. I am truly grateful for the opportunity to work in his lab – Supramolecular Organic Chemistry Group (SOCG). His timely advice, scientific approach, and continuous support have always guided me forward. I deeply appreciate the time he dedicated—despite his busy schedule—to sharpen my research skills and discuss my results. This work would not have been possible without his leadership and motivationAbove all, I am deeply thankful to my parents for their unconditional love, constant encouragement, and unwavering belief in me—they have been my greatest source of strength throughout this journey.

I would also like to extend my heartfelt gratitude to Dr. Sourav Bhowmik, without whose constant guidance, insightful suggestions, and unwavering support this work would not have been possible. I am especially thankful to Mr. Tanmay Rit, whose help during my first lab rotation and throughout my thesis work has been truly invaluable. A special thanks to Ms. Arati Samal and Ms. Anushree Jain for always being there with kind words, mental support, and encouragement. I sincerely thank Mr. Arka Acharyya, who has supported me in every aspect of my research with patience and generosity. I also thank Mr. Santanu Paul, who has helped me at various stages of my work, and other lab members for their support, scientific discussions, and generous sharing of time.

I would also like to thank the Director of IIT Indore, **Prof. Suhas S. Joshi** for allowing me to join this prestigious institute. I am also thankful to the Department of Chemistry and Sophisticated Instrumentation Facility for helping with different aspects of my research.

Dedicated to my father Mr. Swapan Kr
Sarkar and mother Mrs. Mamata Sarkar



Abstract

This study reports the design and synthesis of peptide gels using an oxo-ester-mediated native chemical ligation (NCL) strategy. The approach involves chemo-selective coupling of N-terminal cysteine-containing peptides with C-terminal fluorophenyl esters—specifically, 4-(trifluoromethyl)phenol and 2,3,4,5,6-pentafluorophenol which were successfully incorporated into peptide segments. The ligation reactions proceeded efficiently in aqueous conditions, without requiring external thiol catalysts or protecting groups.

Confocal laser scanning microscopy (CLSM) revealed that the resulting ligated peptides formed entangled nanofibrous networks, creating continuous gel matrices stabilized by covalent and non-covalent interactions such as hydrogen bonding and hydrophobic effects. Rheological analysis confirmed desirable viscoelastic properties, including shear-thinning and thixotropic behavior, with excellent recovery under cyclic stress—highlighting their suitability for injectable and dynamic biomedical applications.

Spectroscopic analyses provided further insight into the assembly process—FTIR and circular dichroism (CD) confirmed β -sheet-rich hydrogen-bonded structures, fluorescence spectroscopy demonstrated the importance of hydrophobic interactions, and NMR verified the chemical integrity of the ligated peptides.

Overall, this work establishes oxo-ester-mediated NCL as a versatile platform for constructing peptide-based nanomaterials. The combination of synthetic control, spontaneous self-assembly, and tunable mechanical properties offer significant potential for the development of next-generation biomaterials for therapeutic, regenerative, and diagnostic applications.



TABLE OF CONTENTS

LIST OF FIGURES	viii-ix
NOMENCLATURE	xi
ACRONYMS	xii
Chapter 1	
1.1 Introduction	1-4
Chapter 2	
2.1 Literature Survey	4-6
2.2 Motivation and Objective	6-7
Synthetic Approach	
Chapter 3	
3.1 Experimental Section	8
Chapter 4	
4.1 Reaction Scheme	9
4.2 Synthesis of compounds	9-18
Chapter 5	
Characterization	19-3
Chapter 6	
6.1 Conclusion	37
6.2 Scope of work	38
References	39-41

LIST OF FIGURES

Figure	Description	Page
		No.
Figure 1	Seleno-ester mediated native chemical ligation	1
	and oxo-ester mediated native chemical	
	ligation	
Figure 2	β-Lactone-mediated native chemical ligation	
		5
Figure 3	Selenoester-mediated native chemical ligation	
	and explore it in molecular self-assembly	5
Figure 4	Thiol - additive free NCL	
		6
Figures 5-16	HPLC, ESI-MS, ¹ H and ¹³ C NMR of	19-24
	compounds 3-5	
Figure 17	HPLC chromatogram of 6a	25
Figure 18	ESI-MS of compound 6a	25
Figure 19	¹³ C NMR (MeOH-d ₄ ,125MHz) spectrum of	26
	compound 6a	
Figure 20	HPLC chromatogram of 6b	26
Figure 21	¹ H NMR (MeOH-d ₄ ,125MHz) spectrum of	27
	compound 6b	
Figure 22	HPLC chromatogram of the NC1 hydrogel and	27
	6a	
Figure 23	Plots of (a) Storage modulus and Loss modulus	
	vs. Strain (%), (b) Storage modulus and Loss	
	modulus vs. Angular frequency, (c) Shear	28
	viscosity vs. Shear rate determined the	
	rheology experiment of NC1 hydrogel	

Figure 24	FTIR spectra of NC1 hydrogel, NC1, Cys and	29
	Pfp	
Figure 25	PXRD data of NC1 hydrogel, NC1 and Cys	30
Figure 26	CD spectrum of NC1 hydrogel, NC1, Pfp and	31
	Cys	
Figure 27	(a) SEM image and (b) CLSM image of NC1	31
	hydrogel	
Figure 28	HPLC chromatogram shows the conversion of	32
	NC2 with the time	
Figure 29	FT-IR spectra of the NC2 hydrogel, Cys and	32
	NC2	
Figure 30	(a) Concentration dependent UV-vis spectra of	
	the $NC2$ (b) The normalized fluorescence	33
	emission spectra of the $NC2$ and $NC2$ hydrogel	
Figure 31	CD spectra of the NC1 hydrogel solution (blue	
	line), NC1 (red line) and Cys (green line)	34
Figure 32	Plots of (a) Storage modulus and Loss modulus	
	vs. Strain (%), (b) Storage modulus and Loss	
	modulus vs. Angular frequency, determined the	35
	rheology experiment of NC1 hydrogel	
Figure 33	The CLSM images of NC2 hydrogel. The scale	
	bar is 5 $\mu m.$ The image was taken using 100x at	36
	z1.0 magnification	

NOMENCLATURE

 \bullet δ Delta (chemical shift)

• nm Nanometer

• mL Milliliter

• ppm Parts per million

• Hz Hertz

• g Gram

• mg Milligram

• °C Degree Celsius

• α Alpha

• γ Gamma

• β beta

ACRONYMS

•	Nmoc	Naphthalene-
	2-methoxycarbonyl	•
•	F	Phenylalanine
•	V	Valine
•	Boc	tert-Butoxy
•	carbonyl	
•	(Boc) ₂ O	tert-Butoxy
•	carbonyl anhydride	
•	CHCl ₃	Chloroform
•	DCM	Dichloromethane
•	DMF	N, N-dimethylformamide
•	DMSO	Dimethyl sulfoxide
•	EtOAc	Ethyl acetate
•	EDC.HCl	N-(3-
	Dimethylaminopropyl)-	N'- ethylcarbodiimide
	hydrochloride	
•	MeOH	Methanol
•	NaOH	Sodium
	Hydroxide	
•	LiOH	Lithium Hydroxide
•	NMR	Nuclear Magnetic Resonance
•	Na_2SO_4	Sodium sulfate
•	TFA	Trifluoroacetic acid
•	TLC	Thin Layer Chromatography
•	NCL	Native ChemicalLigation
•	S	Singlet
•	d	Doublet
•	m	Multiplet
•	J	Coupling constant

CHAPTER 1

1.1 Introduction:

Amino acids, the fundamental building blocks of proteins, consist of three core components: an amino group, a carboxyl group, and a unique side chain (R-group) that determines their specific chemical and physical properties. The 20 naturally occurring amino acids exhibit diverse characteristics, such as hydrophobicity, hydrophilicity, or charge, which enable them to form complex three-dimensional structures when linked together in peptides or proteins.

Peptides, as short chains of amino acids, represent a fundamental class of biomolecules that are critical in regulating and executing diverse biological functions. Each amino acid contains an amino group, a carboxyl group, and a unique side chain that determines its physicochemical properties. When linked through amide bonds, they give rise to peptides and proteins, the core molecular machinery of living systems. Beyond their biological roles, synthetic peptides have emerged as versatile tools in chemistry, biology, and materials science due to their inherent biocompatibility, molecular recognition capabilities, and chemical tunability. Their modularity allows researchers to incorporate functional groups or modifications, facilitating a wide range of biomedical and nanotechnological applications [1-3].

Seleno-ester mediated Native Chemical Ligation (NCL):

$$R_1 \xrightarrow{\text{NS}} SR_4 + H_2 \xrightarrow{\text{NS}} R_3 \xrightarrow{\text{trans-}} R_1 \xrightarrow{\text{thioesterification}} R_3 \xrightarrow{\text{trans-}} R_3 \xrightarrow{\text{intamolecular rearrangement}} R_3 \xrightarrow{\text{rearrangement}} R_1 \xrightarrow{\text{NS}} R_3 + R_4 SH$$

Oxo-ester Mediated Native Chemical Ligation:

$$R_1 \xrightarrow[R_2]{OR_5} + H_2 \xrightarrow[\text{thioesterification}]{R_3} \xrightarrow[\text{thioesterification}]{R_1 \xrightarrow[\text{superposition}]{OR_5}} R_3 \xrightarrow[\text{thioesterification}]{R_1 \xrightarrow[\text{rearrangement}]{OR_5}} R_3 \xrightarrow[\text{thioesterification}]{R_1 \xrightarrow[\text{thioesterification}]{OR_5}} R_3 \xrightarrow[\text{thioesterification}]{OR_5} R_5 \xrightarrow[\text{thioesterificatio$$

Figure 1. Seleno-ester mediated native chemical ligation and oxo-ester mediated native chemical ligation.

One of the primary challenges in peptide-based self-assembly is achieving control over the size, shape, stability, and functional responsiveness of the assembled structures. To address this, various stimuli-responsive designs have been proposed, including pH, temperature-, redox-, and enzyme-sensitive systems ^[7-8]. Among the synthetic techniques used to create such systems, Native Chemical Ligation (NCL) has gained prominence as a highly chemoselective method for peptide bond formation under mild aqueous conditions. First introduced by Kent and colleagues, NCL is a reaction where a peptide bearing a C-terminal thioester reacts with another peptide containing an N-terminal cysteine, leading to the formation of a native peptide (amide) bond. This strategy allows the joining of unprotected peptide segments and has been extensively applied in protein synthesis, semisynthesis, and the construction of post-translationally modified peptides ^[9,10]. The selenoester mediated native chemical ligation is shown in **Figure 1**.

Recent innovations have sought to expand the utility of NCL by replacing the traditional thioesters with alternative activated esters, such as oxo-esters. Oxo-ester-mediated ligation (shown in **Figure 1**) enables broader chemical versatility and potentially eliminates the need for thiol additives, which can complicate purification or interfere with downstream reactions. Moreover, using oxo-esters with strong electron-withdrawing groups at the para position of the phenolic leaving group can significantly enhance the reactivity and efficiency of the ligation reaction. These modifications are especially beneficial in the synthesis of peptide-based materials where post-ligation self-assembly is a key step [11,12].

Peptide self-assembly following NCL provides a seamless route to construct hierarchical nanostructures. The ligated peptides, when appropriately designed, can undergo spontaneous organization into gels or fibrils under physiological conditions. This property is particularly advantageous for creating injectable hydrogels, scaffolds for cell culture, or drug-loaded matrices that respond to environmental triggers. The use of NCL in conjunction with self-assembling sequences thus presents a powerful approach

to designing multifunctional materials that bridge synthetic chemistry and biology [13-15]. To fully characterize and validate such systems, a combination of analytical and spectroscopic techniques is employed. Confocal Laser Scanning Microscopy (CLSM) provides direct visualization of the nanostructures, revealing insights into fiberlike morphology and spatial organization. Rheological studies assess the mechanical properties and response to shear, which are crucial for determining the suitability of these gels for biomedical applications. Spectroscopic analyses such as FTIR and Circular Dichroism (CD) confirm the presence of secondary structural motifs like betasheets, often linked to fibrous peptide assemblies. Furthermore, Nuclear Magnetic Resonance (NMR) spectroscopy is essential for understanding the chemical integrity of the ligated peptides and monitoring post-ligation modifications.

Among the fascinating applications of peptides is their ability to self-assemble into well-defined supramolecular structures, such as nanofibers, nanotubes, ribbons, and hydrogels. This process of self-assembly, governed by non-covalent interactions including hydrogen bonding, hydrophobic effects, van der Waals forces, and π – π stacking, enables the formation of complex architectures from simple peptide sequences. These nanostructures have been explored for applications in drug delivery, tissue engineering, biosensing, and the development of responsive materials. The ability to engineer such materials at the molecular level offers the potential for precision medicine and smart therapeutic platforms ^[4-6].

Desulfurization reactions offer an additional layer of control over the material properties of self-assembled peptides. By selectively converting cysteine and related residues to alanine or valine, one can tailor the hydrophobicity, structural rigidity, and functional behavior of the peptide gels post-assembly [20,22]. This strategy allows researchers to study the role of individual amino acid residues in self-assembly and modulate the material properties without disrupting the primary sequence or backbone structure. Such chemical flexibility is critical in designing next-generation soft materials that can be

adapted for specific functions in drug delivery, wound healing, or cellular engineering [17-19].

In this context, the integration of oxo-ester-mediated NCL (shown in **Figure 1**) with self-assembling peptide chemistry represents a promising avenue for the development of dynamic and responsive biomaterials. This approach leverages precise chemical synthesis with supramolecular assembly to construct systems that are not only structurally robust but also functionally rich. As research progresses, the understanding of structure–function relationships in peptide-based materials will deepen, paving the way for innovations in therapeutic design, diagnostics, and regenerative medicine [22-24]

The following chapters present a detailed account of the strategies employed, the ligation reactions optimized, and the comprehensive characterization of the resulting peptide-based soft materials. By combining principles from organic synthesis, biochemistry, and materials science, this study aims to contribute to the expanding field of peptide-based nanotechnology with a focus on modularity, functionality, and translational potential

CHAPTER 2

2.1 Literature Survey:

NCL has become a cornerstone technique in peptide and protein synthesis due to its ability to form native amide bonds under mild conditions. Since introduced by Kent et al. in the early 1990s, NCL has provided researchers with an efficient way to synthesize peptides without the need for extensive protection groups. This methodology has proven particularly useful for generating large peptides and enabling self-assembly studies.

Recently Xinhao Fan and his co-workers ^[9] (2024) introduced an innovative approach to achieve epimerization-free NCL through β -lactone-mediated ligation [shown in **Figure 2**]. The β -lactone structure provides a constrained

environment that facilitates rapid peptide ligation while preventing detectable epimerization.

Figure 2. β-Lactone-mediated native chemical ligation. ^[9]

This approach demonstrates wide side-chain compatibility and has been effectively utilized to synthesize cyclic peptides and polypeptidyl thioesters, which are challenging to produce using conventional techniques.

Redox-active peptides were synthesized by Rasale and Das ^[11] via selenoester-mediated native chemical ligation (NCL), leading to diverse nanostructures like nanotubes and nanofibrils for soft materials as shown in **Figure 3**.



Figure 3. Selenoester-mediated native chemical ligation and its exploration in molecular self-assembly.^[11]

Shugo Tsuda and his co-workers ^[3] did a study that demonstrates a method for synthesizing peptides which are cystine rich through thiol-additive free NCL [**Figure 4**]. It employs tris(2-carboxyethyl)phosphine (TCEP) as a reductant, enabling producive ligation even at difficult sites like Thr-Cys and Ile-Cys. This direct synthesis combines NCL and oxidative folding, producing high-purity peptides essential for biological studies. The researchers successfully

synthesized protoxin I (ProTx-I), highlighting the method's potential for therapeutic applications.

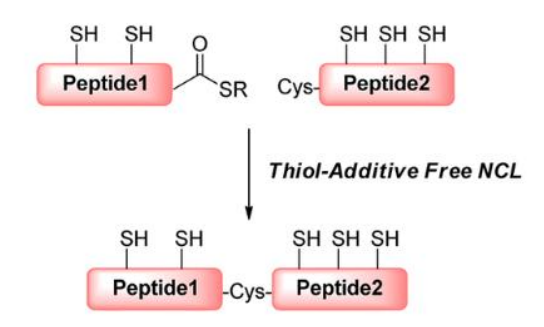


Figure 4. Thiol-additive free NCL [3]

The use of NCL mediated by oxo-ester for self-assembly was highlighted by Rasale and Das ^[9] (2013), who demonstrated that p-NP (p-nitrophenyl) esters could act as effective acyl donors for self-assembly via NCL.

Peptide self-assembly is predominantly driven by non-covalent interactions, including π - π stacking, hydrogen bonding, and hydrophobic effects. Recent research has focused on fine-tuning these interactions to achieve desired material properties. For instance, studies on antimicrobial peptides by Cao *et al.* [19] revealed that aromatic side chains could enhance self-assembly, creating stable nanostructures with applications in drug delivery

Additionally, Xiang *et al.* ^[16] developed peptide-based hydrogels activated by light, showcasing how external stimuli can regulate peptide assembly and disassembly, a feature of significant relevance for biomedical applications. These advancements in stimuli-responsive systems underscore the versatility of peptides in self-assembly.

2.2 Motivation and Objectives:

The study of peptide self-assembly offers significant potential for creating functional nanomaterials with applications in tissue engineering, drug delivery, and biomaterials. NCL (native chemical ligation) is a commonly employed method for peptide synthesis, often utilizing acyl donors such as

thioesters or p-nitrophenyl (p-NP) esters. Now the target is to evolve a simple and systematic method by utilizing native chemical ligation (NCL) mediated by oxo-ester for peptide coupling, followed by self-assembled peptide gel formations. While previous research has focused on using p-nitrophenyl (p-NP) esters [11] as acyl donors, the potential of alternative leaving groups in promoting peptide self-assembly via NCL remains unexplored. In this work, we aim to investigate the use of 4-(trifluoromethyl)phenol, 2,3,4,5,6-pentafluorophenol as novel acyl donors, hypothesizing that these fluorinated phenols could enhance ligation efficiency compared to p-NP esters.

I plan to synthesize amino acids protected by Nmoc and peptides with C-terminal fluorinated phenol esters and study their potential for facilitated self-assembly through native chemical ligation (NCL) utilizing N-terminal cysteine residues. By exploring these modified ligation precursors, I aim to improve peptide coupling efficiency and investigate the construction of organized nanostructures. This research intends to shed light on the effectiveness of these new leaving groups in peptide self-assembly and their potential applications in designing novel biomaterials.

CHAPTER – 3

3.1 Experimental section

Materials required:

The solvents and reagents were purchased from commercially available sources. Alfa Aesar, Sigma Aldrich India, Merck, Spectrochem, and TCI are some available sources.

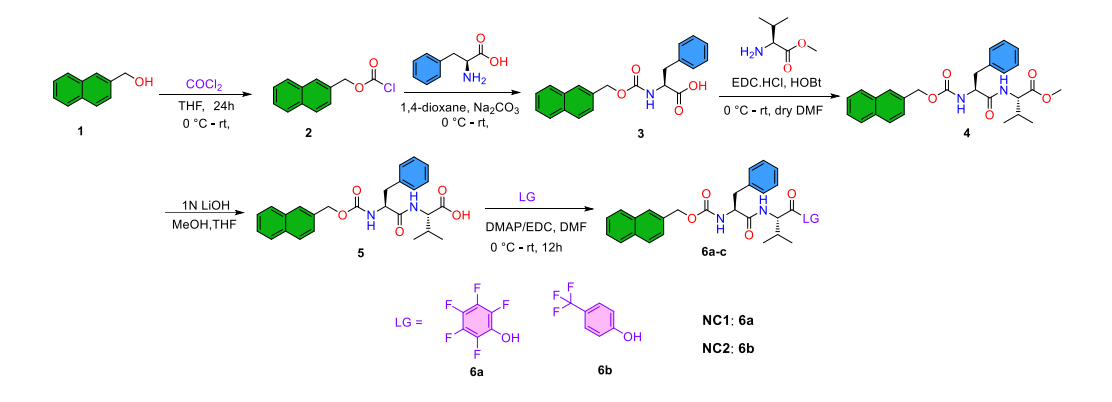
L-Phenylalanine, L-Valine, diethyl ether, EDC.HCl, HOBT, Et₃N, and lithium hydroxide pellets were purchased from the Sisco Research Laboratory. Thionyl chloride and Phosgene was purchased from Spectrochem. DMF and methanol were purchased from Merck, ethyl acetate was purchased from FINAR limited, and petroleum ether was purchased from Advent. After completion of the reaction, silica (230-400 mesh) was used in the flash column to purify the compound with ethyl acetate and petroleum ether as mobile phase. For moisture-sensitive reactions, the dry solvents were used in N₂ gas.

General Procedure:

TLC monitored the course of reactions. NMR spectra were recorded on Bruker Avance (500 MHz) instrument at 25 °C. Mass spectra were set down on the Bruker instrument by using ESI-positive mode. The NMR spectra of all substrates were analyzed using MestReNova software. The NMR samples were prepared in CD₃OD and CDCl₃ solvent.

CHAPTER - 4

4.1 Reaction Scheme:



Scheme 1. Synthetic pathway of **NCs**.

4.2 Synthesis of Compounds:

4.2.1. Naphthalene-2-methyloxy chloroformate [1] synthesis:

At first 0.5 g of 3.16 mmol 2-naphthalene methanol was dissolved in 14.3 mL of dry THF then stirred at ice-cold condition. After 3-5 mins 3.92 mL of 7.9 mmol phosgene was added to the mixture. Then left to stir for 48 hours. The completion of the reaction was tracked by TLC. Upon completion, excess amount of phosgene was eliminated by trapping with NaOH under low vacuum. Then it was further concentrated under rota and oily product found. Then with addition of little amount of hot hexane solid white crystalline product was formed. Yield: 91% (634 mg).

4.2.2. Synthesis of ((naphthalen-2-ylmethoxy)carbonyl)-L-phenylalanine [2]:

Reagents	mol. wt.(g/mol)	equiv. mmol.		weight(g)
Nmoc-Cl	220.65	1	8.34	1.85
F-OH	165.19	2	16.7	2.77

At first, 1.85 g of 8.3 mmol was dissolved in 10 mL of 1,4-dioxane and stirred at 0°C then, 13 mL of 1M NaOH solution was added to the reaction mixture. After 5 mins 2.77 g, 16.7 mmol Naphthalene-2-methoxychloroformate was added and stirred for 12h at rt. After completion of the reaction, required amount of water was added for dilution, and dioxane was dispersed using rotavapor. Then after washing the aqueous layer with DEE, it was acidified with 2N HCl solution. Then extracted 3 times using EtOAc. With addition of Na₂SO₄ organic layer was concentrated in rotavapor to give oily product. Yield: 86% (2.4g). 1 H NMR (CDCl₃, 500MHz) δ : 3.09-3.26 (m, 2H), 4.71 (t, 1H), 5.27 (s, 2H), 7.15-7.43 (m, 3H), 7.43 (s, 1H), 7.48 (m, 2H), 7.82 (s,1H), 7.89 (m, 3H); 13 C NMR (MeOH- 4 4, 125MHz) δ :37.18, 55.46, 66.26, 125.15, 125.45, 125.77, 125.85, 125.15, 126.37, 127.39, 127.6, 127.78, 128, 128.04, 128.89, 129.13, 133.1, 133.22, 137.12, 157.05, 173.89. LCMS (ESI) m/z (M + Na) $^{+}$: 372.1209.

4.2.3. Synthesis of (S)-1-methoxy-3-methyl-1-oxobutan-2-aminium chloride (V-OMe):

OH SOCI₂
MeOH, 0°C-rt

Wh₂

Wh₃CI
$$\Theta$$

2.0 g of L-Valine was taken in a round-bottom (R.B.) flask, and methanol (25 mL) was added. The reaction mixture was cooled in an ice bath with continuous stirring, and 3.46 mL of thionyl chloride(SOCl₂) was added dropwise. The resulting mixture was stirred at room temperature overnight. After completion of the reaction, the solvent was removed under reduced pressure using a rotary evaporator. To neutralize any residual HCl vapours, a small amount of aqueous NaOH or solid Na₂CO₃ was added to the collection flask of the rota prior to evaporation. An oily residue was obtained, to which a small amount of diethyl ether was added. Upon addition, the product solidified to form a white solid. The solid was collected and dried to yield the methyl ester of S-valine as a white solid in 91% yield.

4.2.4. Synthesis of methyl ((naphthalen-2-ylmethoxy)ca:rbonyl)-L-phenylalanyl- valinate [3]:

Reagents	mol. wt.(g/mol)	equiv.	mmol.	weight(g)
Nmoc-F-OH	335.36	1	4.2	1.4
EDC.HCl	191.7	1.1	4.6	0.88
HOBt	135.12	1.1	4.5	0.62
V-OMe	V-OMe 167.07		8.3	1.39

At first, 1.4 g of 4.2 mmol Nmoc-F-OH was dissolved in 5mL of dry DMF, the R.B. was covered with an Al-sheet to isolate from direct light and stirring was continued at 0°C. Then 0.88 g of 4.6 mmol of EDC.HCl followed by HOBt (0.62 g, 4.5 mmol) were added into the mixture at ice-cold stirring condition. After 10 mins 1.39 g of 8.3 mmol neutralized valine methyl ester was added into the mixture and stirred 12h at rt.

When the reaction was completed, reaction mixture was diluted with EtOAc, then EtOAc layer was washed with 1(N) HCl (2 times x 20 mL) followed by Na₂CO₃ (2 times x 20 mL) and Brine solution (2 times). Then Na₂SO₄ added for drying organic layer and evaporated under Rota vapour to get the product. Yield: 83% (1.56g) ¹H NMR (CDCl₃, 500MHz) δ: 0.76-0.82 (dd, 6H), 2.04-2.08 (m, 1H),3.04-3.11 (m, 2H), 3.66 (s, 3H), 4.44-4.46 (d,1H), 5.25 (t, 1H), 5.26-5.30 (s, 2H), 7.21-7.25 (m. 6H), 7.41-7.43 (m, 1H), 7.49-7.50 (m, 2H), 7.50-7.84 (m, 4H); ¹³C NMR (CDCl₃, 125 MHz) δ: 31.21, 38.32, 52.11, 56.27, 57.32, 67.24, 125.75, 126.25, 126.27, 127.06, 127.17, 127.7, 128.02, 128.36, 128.73, 129.34, 133.14, 133.21, 133.58, 136.29, 155.99, 170.75, 171.72; LCMS (ESI) m/z (M + Na)⁺: 485.2256.

4.2.5. Synthesis of ((naphthalen-2-ylmethoxy)carbonyl)-L-phenylalanyl-L-yaline[4]:

Compound 4 (500 mg, 1.08 mmol) was dissolved in a 1:1 mixture of tetrahydrofuran (THF) and methanol (MeOH). To this solution, 4 mL of 1N lithium hydroxide (LiOH) was added gradually with stirring at room temperature. The reaction progress was monitored by thin-layer chromatography (TLC). After completion of the reaction, methanol was evaporated under reduced pressure, resulting in a solid residue. This residue was dissolved in deionized water and washed with diethyl ether to remove organic impurities. The aqueous phase was then acidified by the slow addition of 1N hydrochloric acid (HCl) until it reached an acidic pH. The resulting product was extracted using ethyl acetate, and the organic layer was dried over anhydrous sodium sulfate (Na₂SO₄), followed by concentration under vacuum resulting in a white solid product. Yield: 92% (0.445g), ¹H NMR (MeOH-d₄, 500 MHz) δ: 0.67-0.86 (m,6H), 1.18-1.3 (m,1H), 2.81-2.94 (m,2H), 3.28 (d, 2H), 4.41-4.42(t, 1H), 5.1 (s, 2H), 7.13-7.21 (m, 4H), 7.35-7.44 (m, 2H), 7.70-7.76 (m, 4H), 7.78-7.93 (m, 2H); 13 C NMR (MeOH- d_4 , 125MHz) δ : 37.1, 37.64, 55.46, 54.11, 55.46, 66.26, 125.15, 125.77, 125.85, 126.16, 126.37, 126.37, 127.29, 127.6, 127.79, 128.01, 128.04, 128.9, 129.13, 133.1, 134.22, 136.77, 137.12, 157.05, 173.9, 174.22; LCMS (ESI) m/z (M - Na)⁻: 447.2233.

4.3.6. Synthesis of perfluorophenyl(naphthalen-2-ylmethoxy)carbonyl)-L-phenylalanyl-L-valinate (6a/NC1):

Optimization Table:

Reactants	Reagents	Solvent	Temperature	Time	Yield (%)
	EDC.HCl; HOBt	Dry DMF	0 °C-rt	12 h	No Reaction
Nmoc-Phe-V-OH (compound 5 of	DMAP; EDC.HCl; HOBt	Dry DMF	0 °C-rt	24 h	No Reaction
Figure 4)	ClCO ₂ Et; NMM	Dry THF	0 °C-rt	12 h	No Reaction
	SOCl_2	Dry THF	0 °C-rt	24 h	No Reaction
Pentafluorophenol	ClCO ₂ Et; Et ₃ N	Dry THF	-15 °C-rt	<mark>4 h</mark>	<mark>44%</mark>
	HATU; DMAP	Dry DMF	0 °C-rt	12 h	No Reaction
	CICO ₂ Et; NMM	Dry THF	-15 °C-rt	6 h	28%

Reaction Scheme:

Reagents	mol.wt.(g/mo	equiv.	mmol.	weight	density(g/mL)	vol.(μL)
	1)			(g)		
Nmoc-F-V-	448.2	1	0.995	466	-	-
ОН						
Et ₃ N	101.19	1	0.995	100.69	0.92	109.44
pFP	184.07	2	1.99	366.33	-	-
ClCO ₂ Et	108.52	1	0.995	107.98	1.13	95.55

Experimental Procedure:

Nmoc-Phe-V-OH (446 mg, 0.995 mmol) in 50 mL THF was added with 0.995 mmol, $109.48~\mu L$) Et₃N, 105.15~mL of ClCO₂Et was added to the reaction mixture at -15 °C and stirred it for 10 min. Pentafluorophenol (95.56 mg) was added to the reaction mixture. The solution was kept for 30 min at -10 °C with stirring. The reaction mixture was stirred for 1h at room temperature. 20 mL water was added. THF was evaporated in vacuum and the residue was dissolved in ethyl acetate. The solution was washed with saturated NaHCO₃ solution and brine water. The ethyl acetate layer was extracted and dried over Na₂SO₄. It was concentrated in vacuum and covered with a layer of petroleum ether. The compound was obtained as white solid. Yield = 44%. The compound was characterised using ESI-MS, 13 C NMR and HPLC chromatogram.

4.3.6. Synthesis of perfluorophenyl(naphthalen-2-ylmethoxy)carbonyl)-L-phenylalanyl-L-valinate (6b/NC2):

Optimization Table:

Reactants	nts Reagents		Temperature	Time	Yield (%)
	EDC.HCl; HOBt	Dry DMF	0 °C-rt	12 h	No Reaction
Nmoc-Phe-V-OH	DMAP; EDC.HCl; HOBt	Dry DMF	0 °C-rt	24 h	27%
(compound 5 of Fig A)	ClCO ₂ Et; NMM	Dry THF	0 °C-rt	12 h	No Reaction
+ 4-	SOCl ₂	Dry THF	0 °C-rt	24 h	No Reaction
(trifluoromethyl)phenol	CICO ₂ Et; Et ₃ N	Dry THF	-15 °C-rt	4 h	41%
	HATU; DMAP	Dry DMF	0 °C-rt	12 h	No Reaction
	ClCO ₂ Et; NMM	Dry THF	-15 °C-rt	6 h	26%

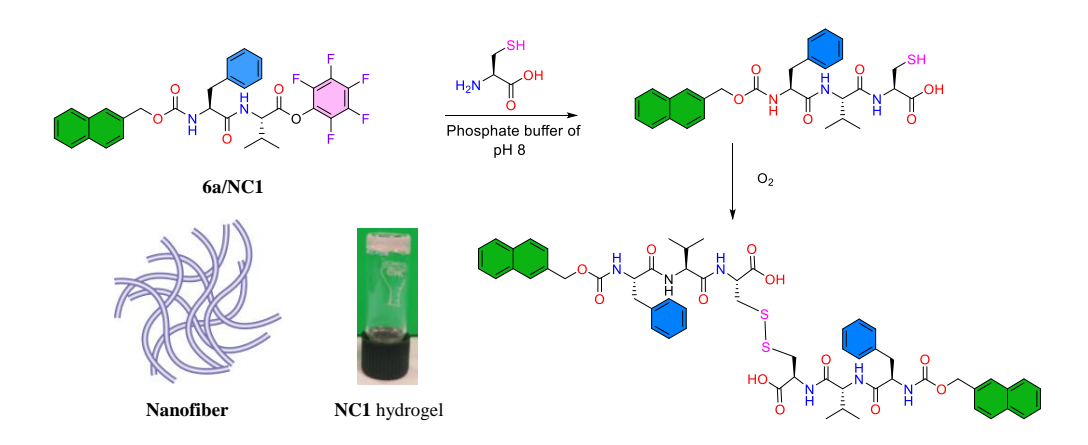
Reaction Scheme:

Reagents	mol. wt.(g/mo l)	equiv.	mmol.	weight (mg)	density(g/ mL)	vol.(μL)
Nmoc-F-V-OH	448.2	1	0.66	300	-	-
Et ₃ N	101.19	1	0.66	67.74	0.92	73.63
4-(trifluoromethyl)phenol	162.11	2	1.33	217.04	-	-
ClCO₂Et	108.52	1.1	0.73	79.88	1.13	70.69

Experimental Procedure:

At first, Nmoc-Phe-V-OH (300 mg, 0.66 mmol) was dissolved in 50 mL THF and 0.66 mmol Et₃N, 70.69 μ L of ClCO₂Et was added to the reaction mixture at -15 °C and stirred it for 10 min. 4-(trifluoromethyl)ophenol (217.04 mg) was added to the reaction mixture. The solution was kept for 30 min at -10 °C with stirring. The reaction mixture was stirred for 1h at room temperature. 20 mL water was added. THF was evaporated in vacuum and the residue was dissolved in ethyl acetate. The solution was washed with saturated NaHCO₃ solution and brine water. The ethyl acetate layer was extracted and dried over Na₂SO₄. It was concentrated in vacuum and covered with a layer of petroleum ether. The compound was obtained as white solid. Yield = 41%. The compound was characterised using ¹H NMR and HPLC chromatogram.

4.4 Synthesis of NC1 Hydrogel:

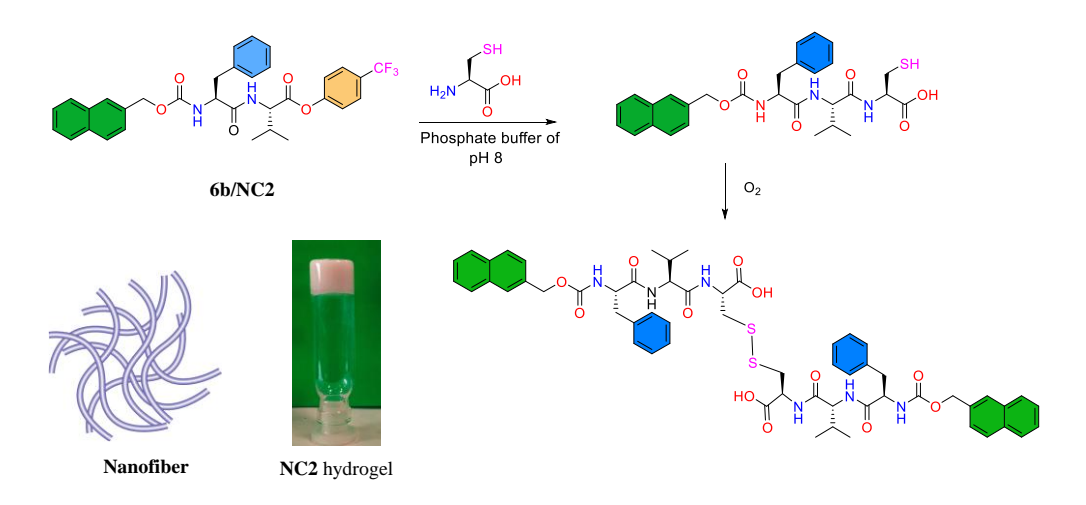


Scheme 2. Synthetic pathway of NC1 hydrogel

Synthetic Procedure of NC1 Hydrogel:

Upon exposure to air, NC1 undergoes oxidation to yield disulfide 1b, which leads to the formation of a self-supporting hydrogel. Initially, all synthesized compounds were analyzed using HPLC. For the gelation study, compound **6a** (0.9 wt%) was first dissolved in 100 μ L of methanol, followed by the gradual addition of a cysteine solution prepared in phosphate buffer (900 μ L, pH 7.5–8). The mixture was incubated at 80 °C for 15 minutes under an inert atmosphere (see **Scheme 2**). Hydrogel formation was verified through the vial inversion test. Notably, HPLC analysis confirmed the presence of the expected product.

4.5 Synthesis of NC2 Hydrogel:



Scheme 3. Synthetic pathway of NC2 hydrogel

Synthetic Procedure of NC2 Hydrogel:

Exposure of NC2 to air led to its oxidation into the disulfide-linked compound 1b, which subsequently formed a self-supporting hydrogel. Preliminary analysis of all compounds was performed using high-performance liquid chromatography (HPLC). For hydrogel preparation, compound **6b** (0.9 wt%) was first dissolved in 100 μ L of DMSO, followed by the gradual addition of 900 μ L of a cysteine-containing phosphate buffer (pH 7.5–8). Within 3–5 minutes, gelation occurred, as shown in **Scheme 3** Hydrogel formation was further validated through the vial inversion test. Notably, HPLC analysis confirmed the formation of the desired product.

CHAPTER - 5

5.1 Characterization of Nmoc-F-OH(compound-3):



Figure 5. HPLC Chromatogram of compound 3

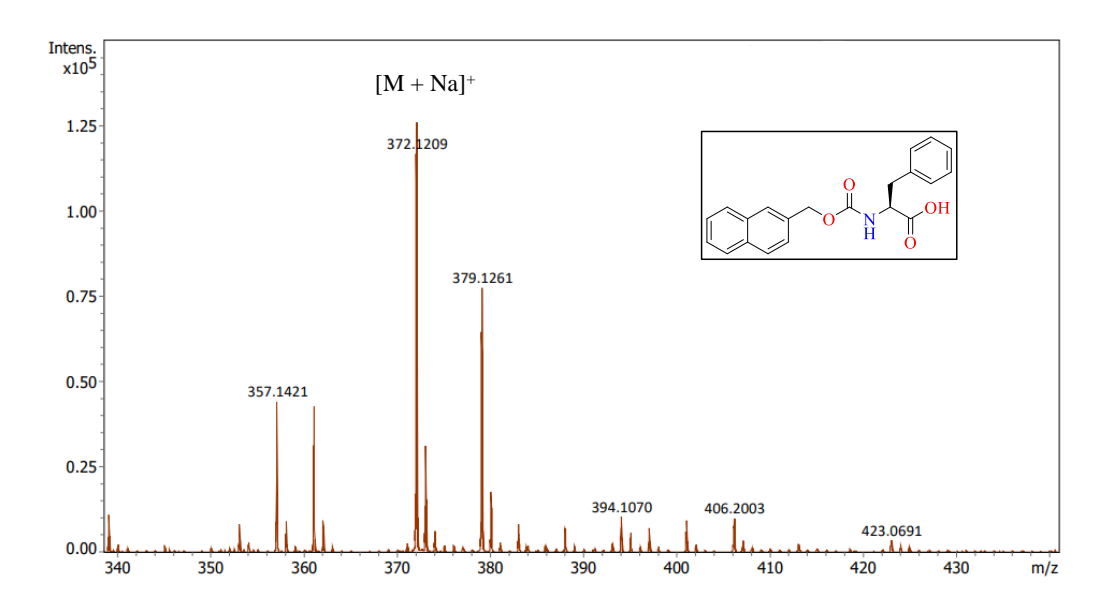


Figure 6. ESI-MS spectrum of Nmoc-F-OH (compound 3)

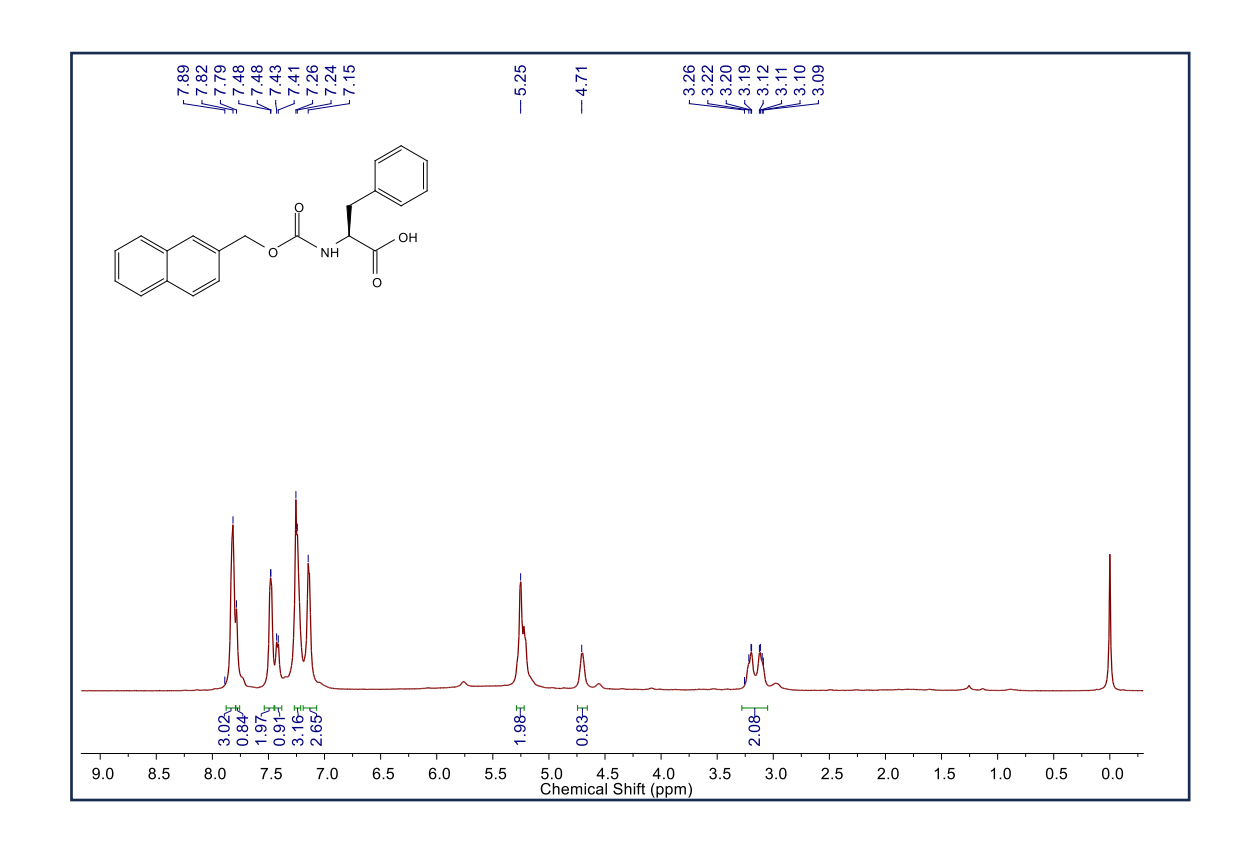


Figure 7. ¹H NMR (CD₃OD, 500 MHz) spectrum of Nmoc-F-OH (compound

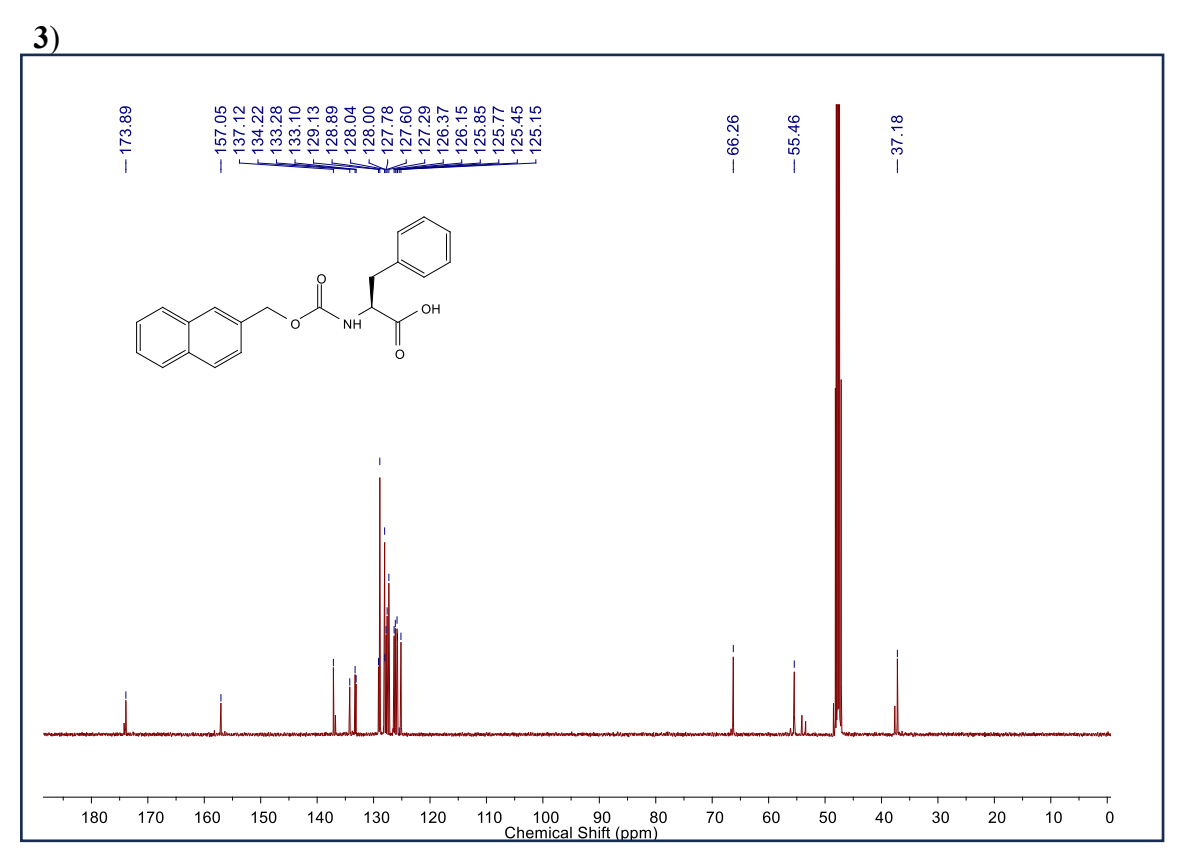


Figure 8. ¹³C NMR (CD₃OD, 500MHz) spectrum of Nmoc-F-OH (compound **3**)

5.2 Characterization of Nmoc-F-V-OMe(compound-4):



Figure 9. HPLC Chromatogram of compound 4

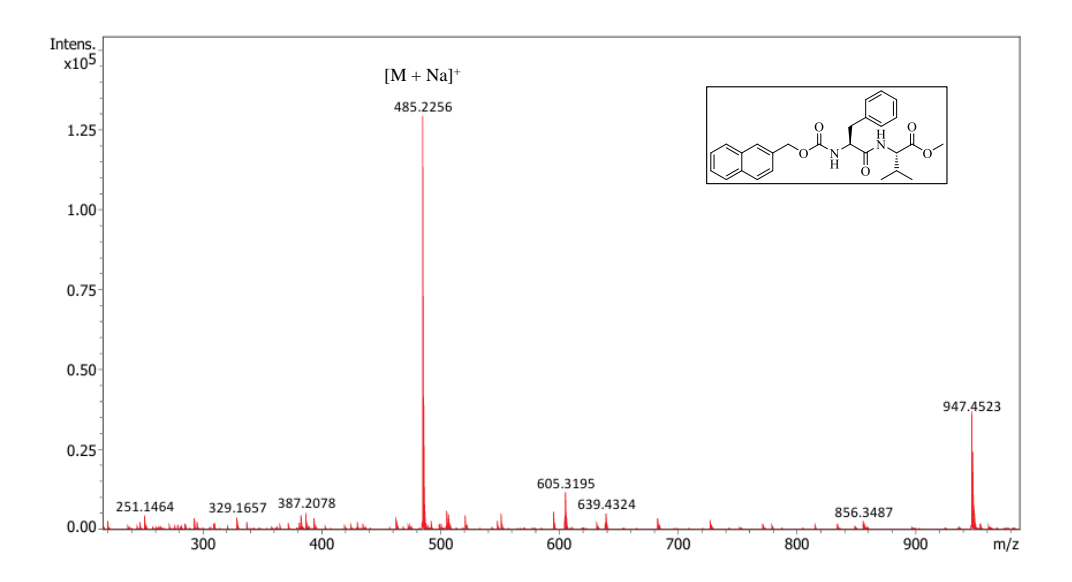


Figure 10. ESI-MS spectrum of Nmoc-F-V-OMe (compound 4)

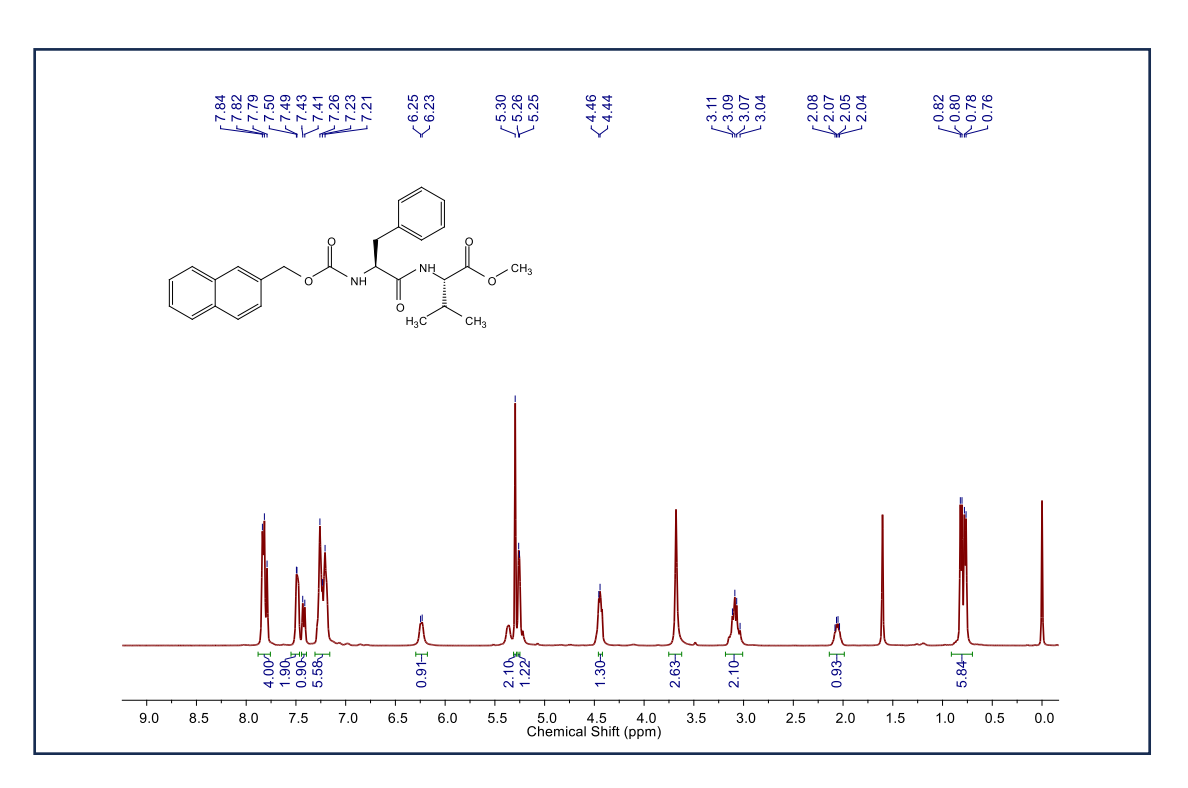


Figure 11. ¹H NMR (CDCl₃, 500 MHz) spectum of Nmoc-F-V-OMe (compound **4**)

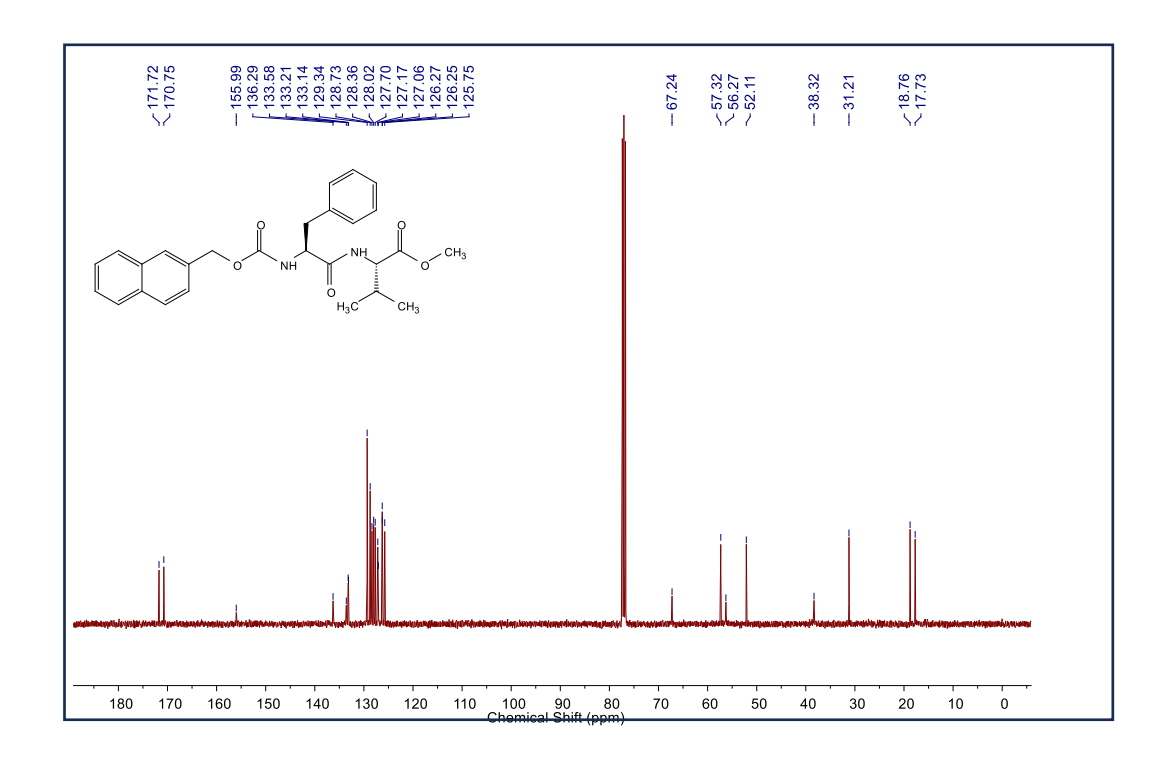


Figure 12. ¹³C NMR (CDCl₃, 125 MHz) spectrum of Nmoc-F-V-OMe (compound **4**)

5.3 Characterization of Nmoc-F-V-OH (compound-5):



Figure 13. HPLC Chromatogram of compound 5

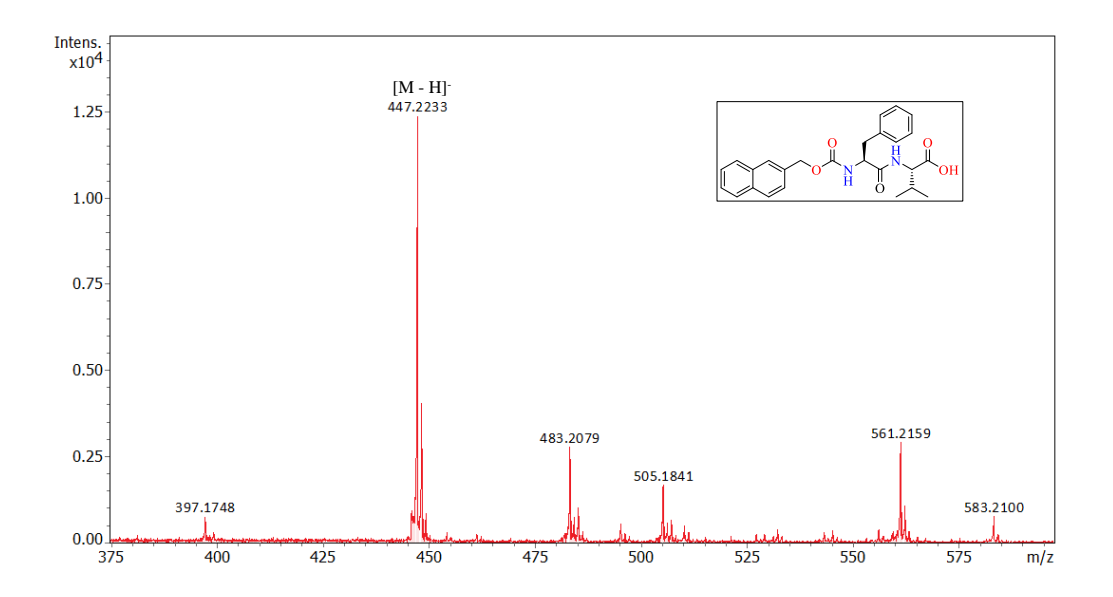


Figure 14. ESI-MS spectrum of Nmoc-F-V-OH (compound 5)

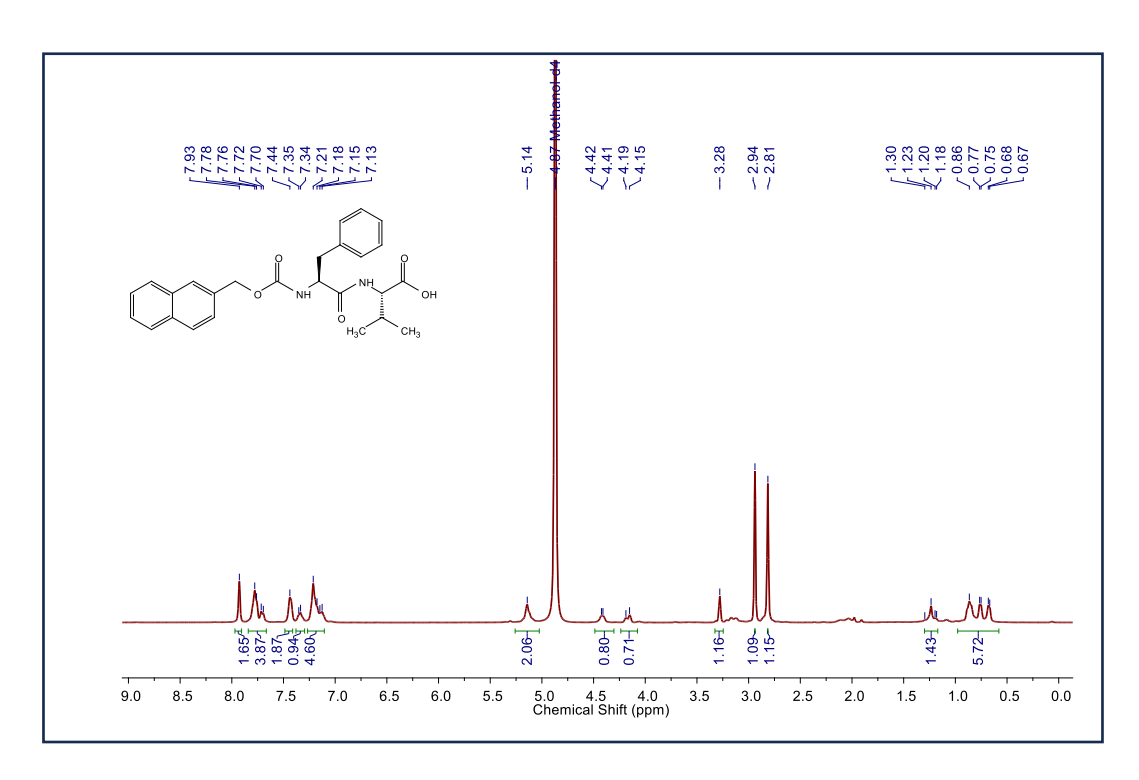


Figure 15. ¹H NMR (CD₃OD, 500 MHz) spectrum of Nmoc-F-V-OH (compound **5**)

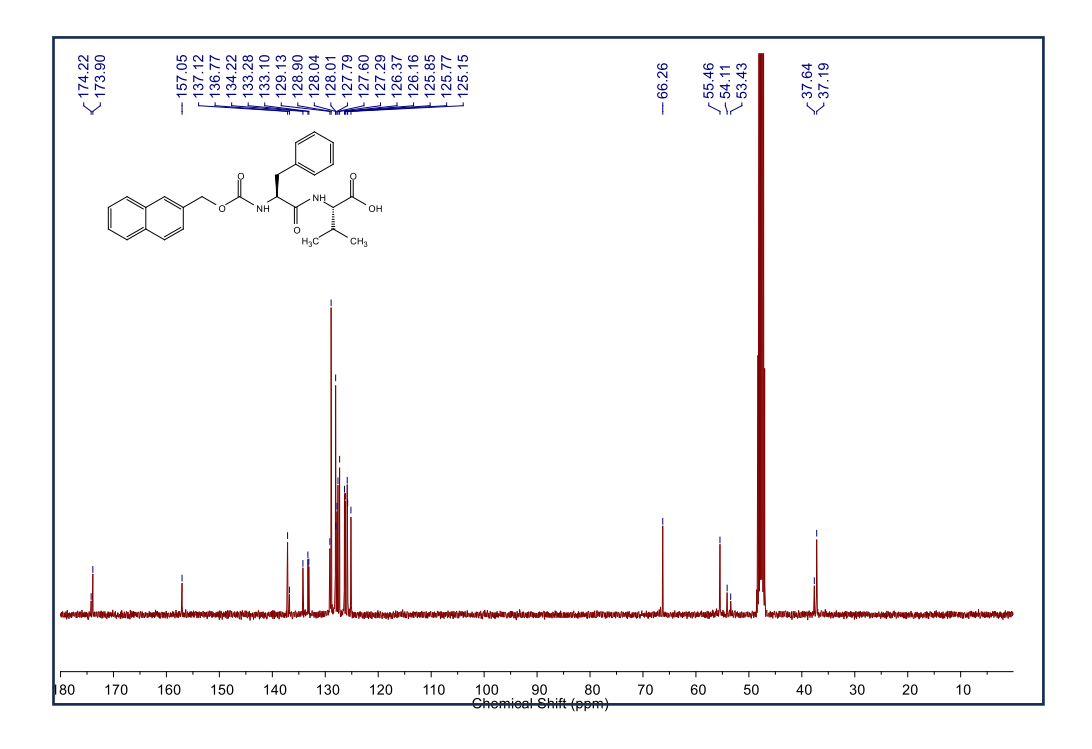


Figure 16. ¹³C NMR (MeOH-*d*₄,125MHz) spectrum of Nmoc-F-V-OH (compound **5**)

5.4 Characterization of Compound 6a:

HPLC Analysis:



Figure 17. HPLC chromatogram of 6a

ESI-MS spectra:

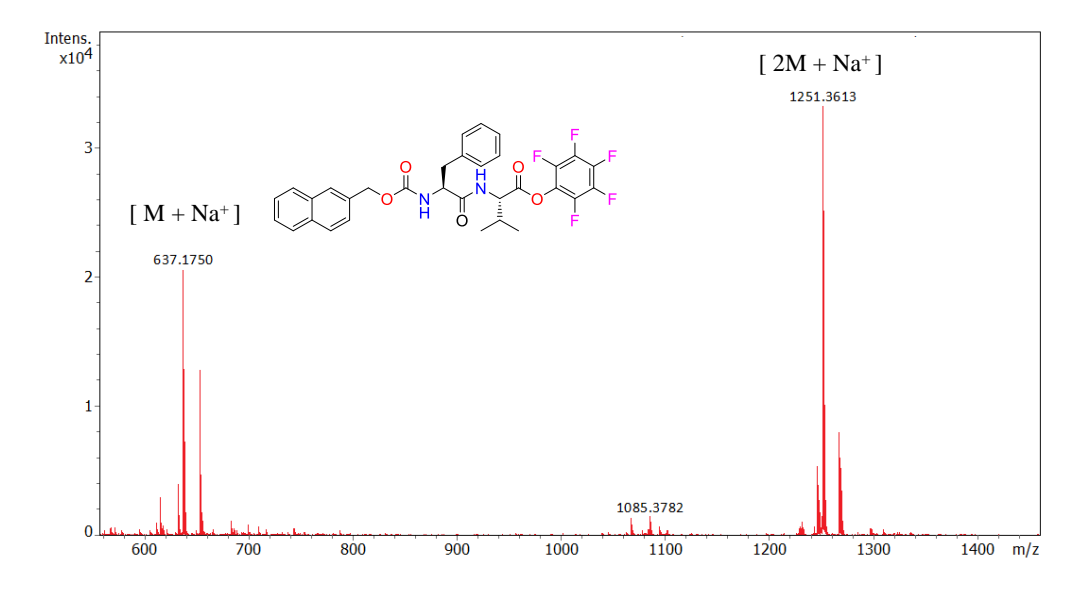


Figure 18. ESI-MS spectrum of 6a

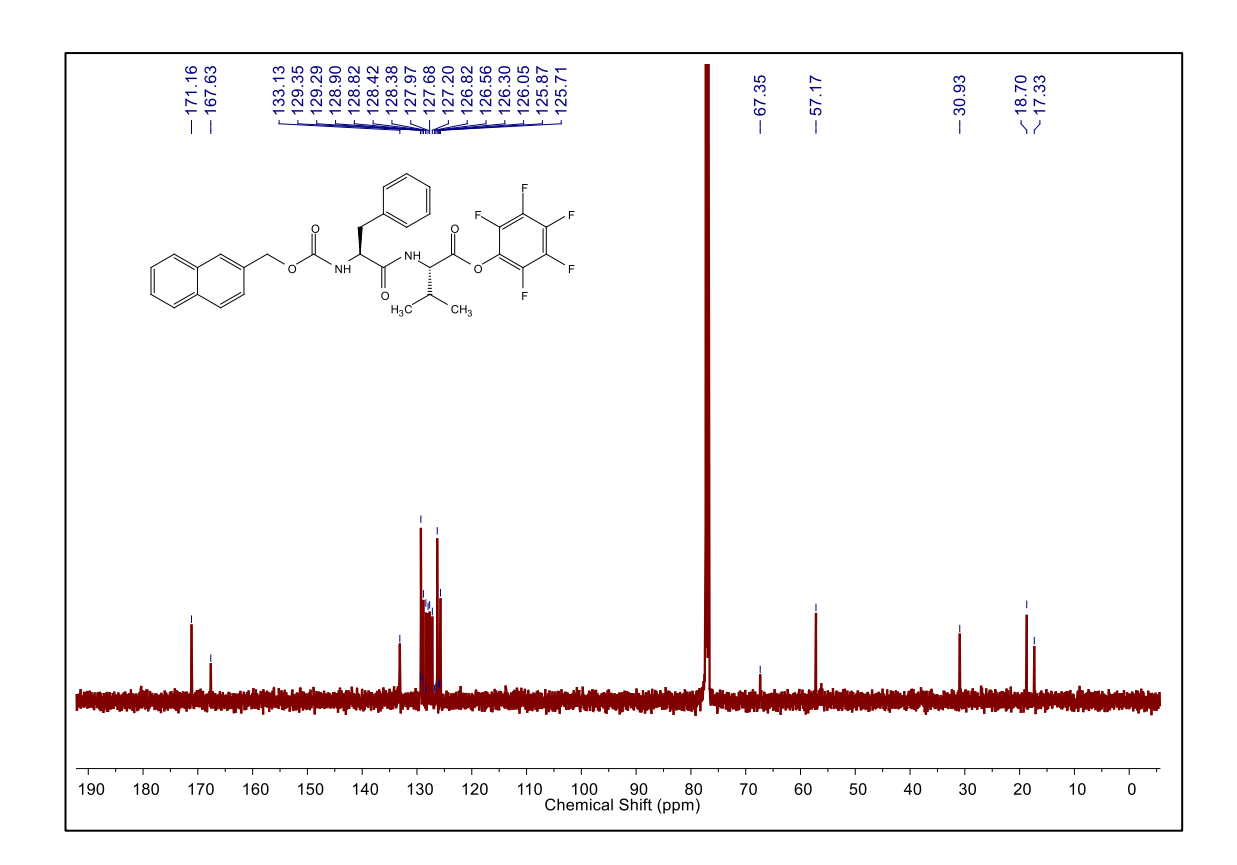


Figure 19. ¹³C NMR (CD₃OD, 125 MHz) spectra of 6a

5.5 Characterization of Compound 6a:

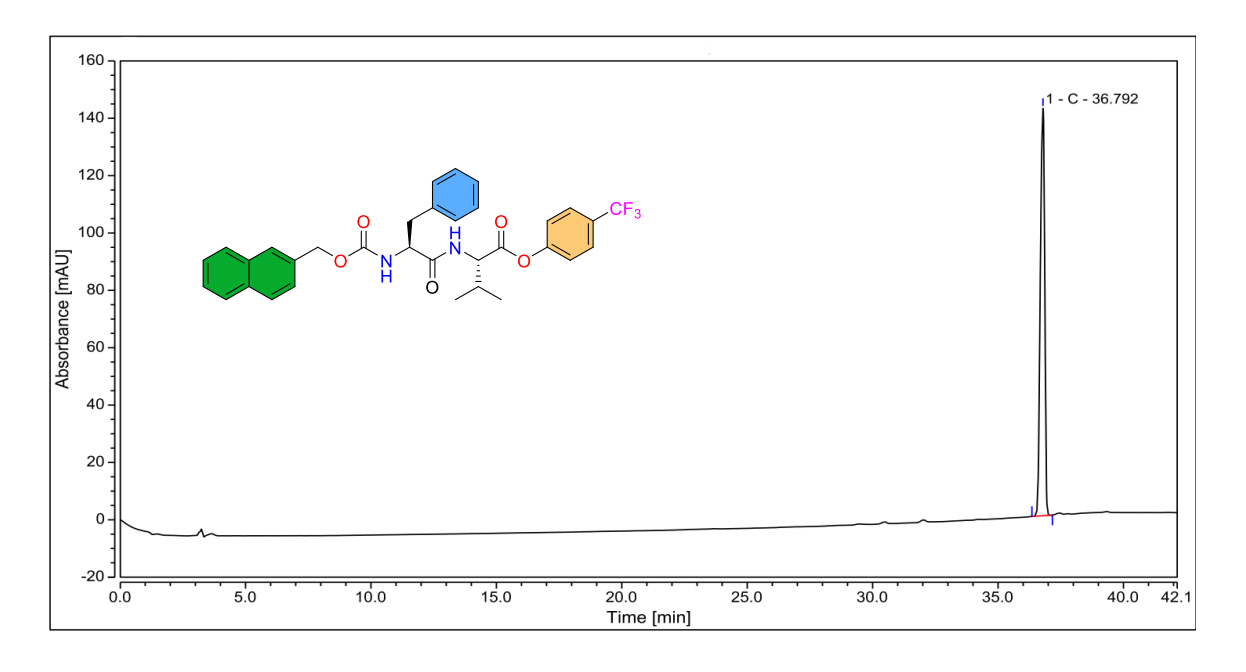


Figure 20. HPLC chromatogram of 6b

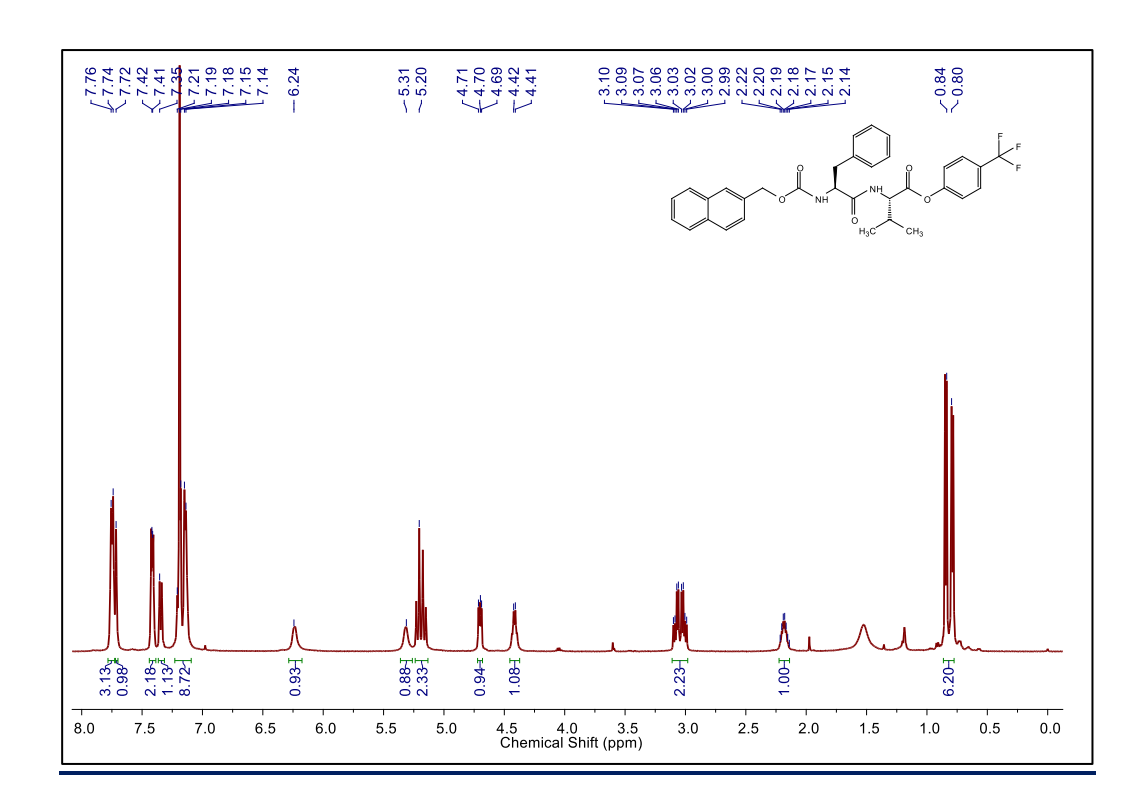


Figure 21. ¹H NMR (CD₃OD, 500 MHz) spectrum of **6b**

5.6 Characterisation of NC1 Hydrogel:

HPLC Analysis:

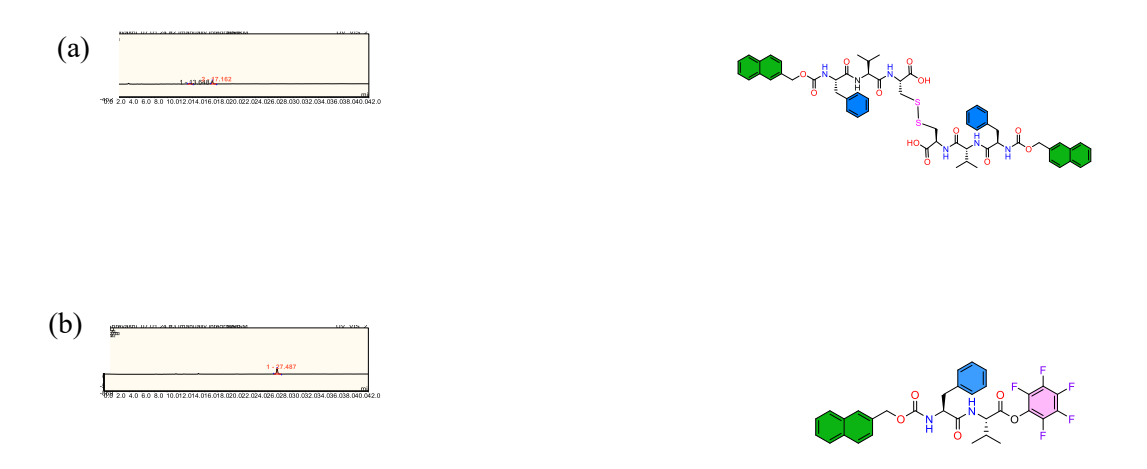


Figure 22. HPLC chromatogram of the (a). NC1 hydrogel and (b). 6a

Rheological Study:

Rheological studies were conducted at 25 °C using an Anton Paar Physica MCR 301 Rheometer. To assess the viscoelastic characteristics of the hydrogel, both the storage modulus (G') and loss modulus (G") were recorded. Freshly prepared hydrogel samples were loaded onto the rheometer plate, and a solvent trap was employed to maintain hydration throughout the analysis. A parallel plate geometry with a 25 mm diameter and a set gap of 0.5 mm was utilized. The plots in **Figure 23a and 23b** show that the viscous modulus (G") is comparatively lower than the elastic modulus (G'), thereby confirming the gel state of the swelled **NC1**. The increasing nature of both moduli against frequency is also evident from **Figure 23a**), which suggests the elastic nature of the **NC1** hydrogel. **Figure 23c** shows that the shear viscosity of the **NC1** hydrogel decreases as the shear rate increases, signifying its pseudo plastic (shear thinning) behaviour.

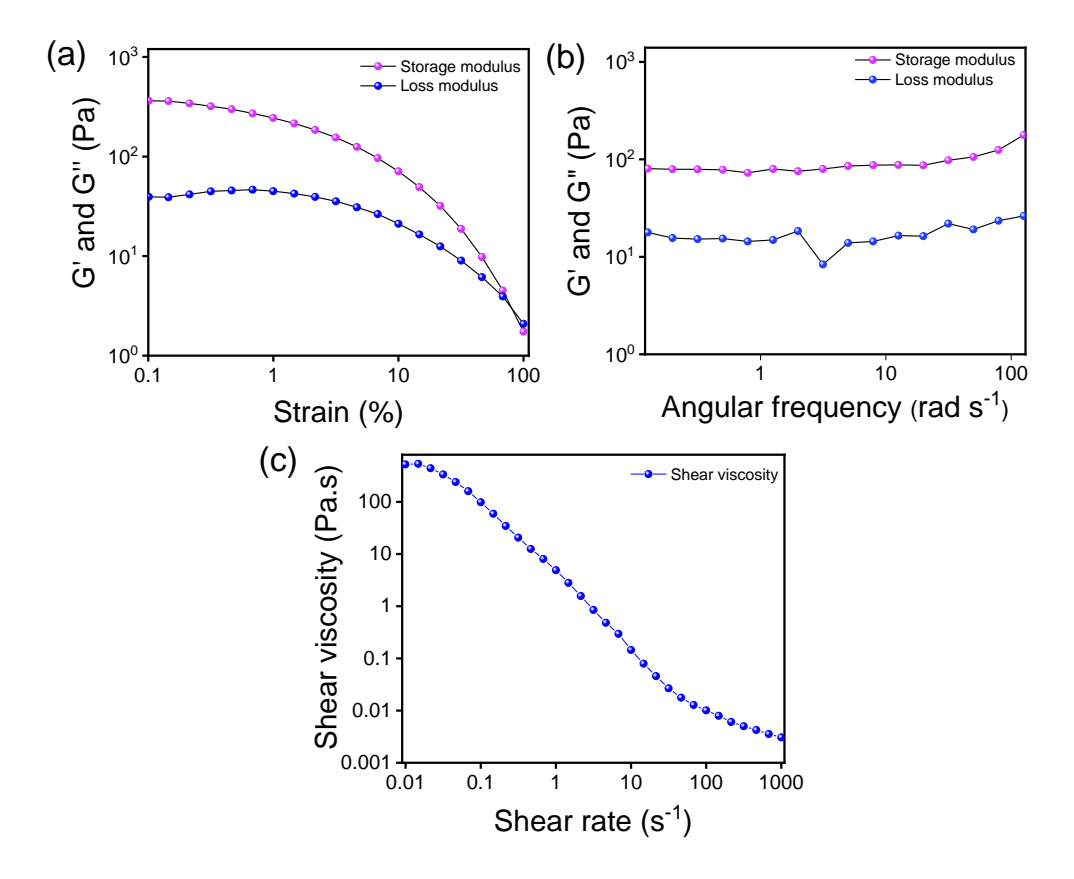


Figure 23. Plots of (a) Storage modulus and Loss modulus vs. Strain (%), (b) Storage modulus and Loss modulus vs. Angular frequency, (c) Shear viscosity vs. Shear rate determined the rheology experiment of **NC1** hydrogel.

FT-IR analysis:

Fourier-transform infrared (FTIR) spectra were recorded using a Bruker Tensor 27 spectrophotometer equipped with ZnSe windows. Gel samples were sandwiched between ZnSe crystal plates and analyzed over a spectral range of 500–4000 cm⁻¹. Each spectrum was collected with 64 scans at a resolution of 4 cm⁻¹ and a data interval of 1 cm⁻¹. The spectra of **NC1** hydrogel was recorded shown in **Figure 24.** For comparison, FT-IR spectra of both **NC1** and Scysteine (**Cys**) were collected. The **NC1** hydrogel sample showed prominent amide I bands at 1607 and 1689 cm⁻¹, indicative of β-sheet formation through peptide self-assembly. A broad absorption band in the region of 2908–3139 cm⁻¹ was also observed, corresponding to N–H stretching vibrations associated with hydrogen bonding.

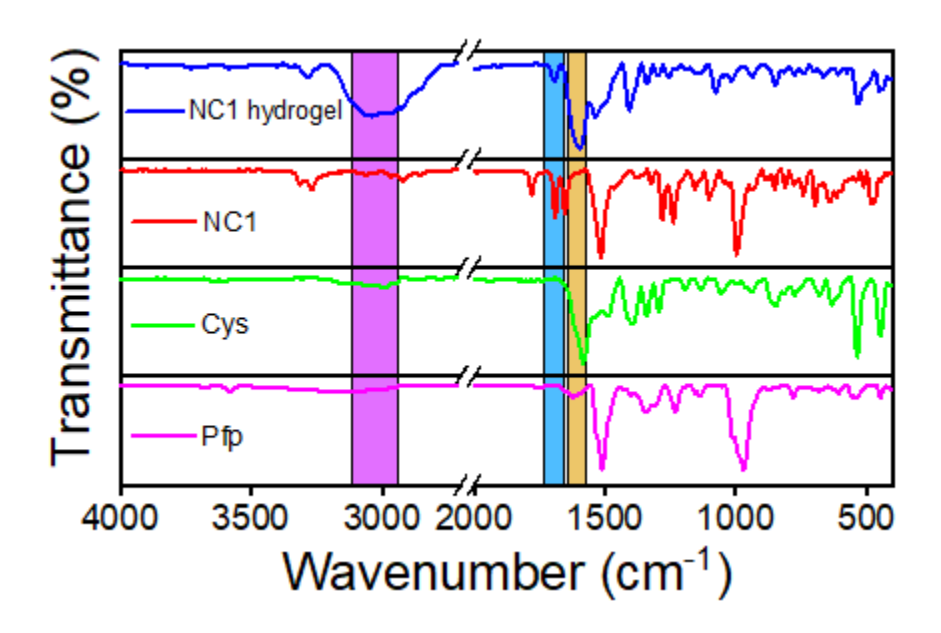


Figure 24. FTIR spectra of NC1 hydrogel, NC1, Cys and Pfp.

Powder X-ray Diffraction (PXRD) Analysis:

At first, the **NC1** hydrogel was lyophilized, and its Powder X-ray Diffraction (PXRD) patterns were recorded along with those of **NC1** and S-cysteine. The measurements were conducted using a Rigaku SmartLab automated multipurpose X-ray diffractometer with a Cu Kα radiation source (wavelength: 0.154 nm) at 25 °C. For PXRD analysis, the samples were placed on a glass

plate. The X-rays were generated using a sealed tube and detected with a high-speed silicon strip-based detector (Scintillator NaI photomultiplier detector).

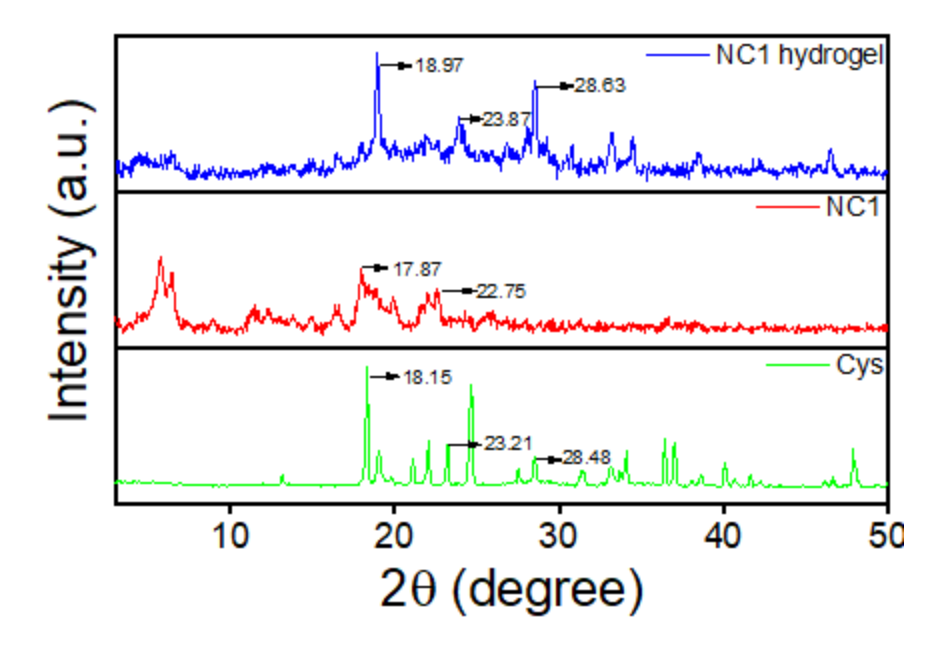


Figure 25. PXRD data of NC1 hydrogel, NC1 and Cys

Circular Dichroism Analysis of Hydrogel:

Circular dichroism (CD) spectroscopy was employed to investigate the secondary structure of peptides in the gel phase. Measurements were conducted at 25 °C using a JASCO J-815 spectropolarimeter equipped with a 1 mm path length quartz cuvette. Spectra were recorded over the wavelength range of 190–260 nm, with a data interval of 0.1 nm and a scan speed of 20 nm/min. For comparison, CD spectra of NC1, cysteine, and pentafluorophenol were also obtained under identical conditions. The CD spectrum of the hydrogel exhibited a characteristic positive band at 208 nm and a negative band at 221 nm, indicative of β -sheet formation. In contrast, these features were absent in the spectra of the individual gelator components. These results suggest the emergence of supramolecular organization and β -sheet structures upon gelation, as illustrated in Figure 26.

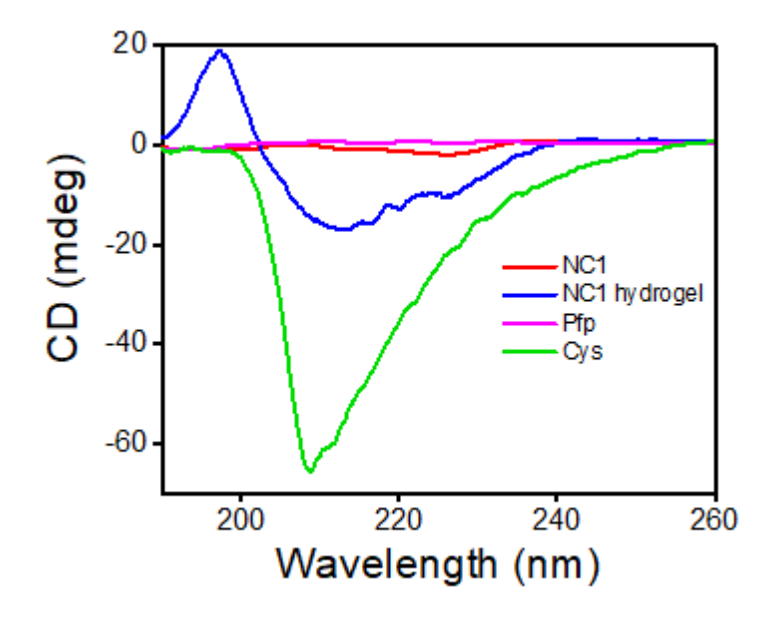


Figure 26. CD spectrum of NC1 hydrogel, NC1, Pfp and Cys.

FE SEM analysis:

The self-assembled morphology of the **NC1** hydrogel, was systematically characterized using advanced microscopic techniques, including field emission scanning electron microscopy (FESEM) and confocal laser scanning microscopy (CLSM). 1mL of 1 mM sample was prepared in eppendorf from 20 mM stock. Then sample was prepared on glass slide by drop-casting and Proceed for the SEM and CLSM analysis. The **NC1** shows fiber like morphology shown in **Figure 27a**.

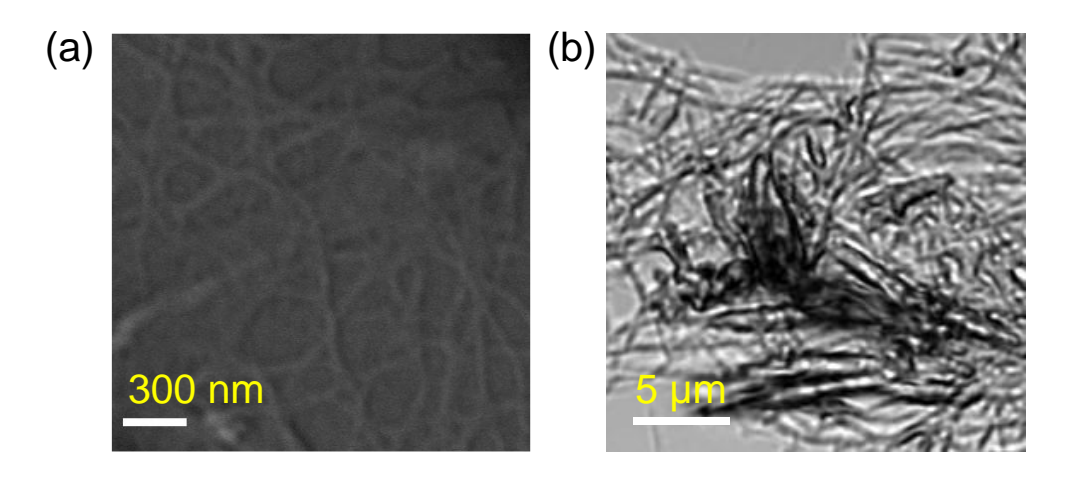


Figure 27. (a) SEM image and (b) CLSM image of NC1 hydrogel

CLSM image also support the observation obtained from the SEM. It also demonstrate the presence of the nanofiber morphology inside the NC1 hydrogel (Figure 27b).

5.7 Characterisation of NC2 Hydrogel:

HPLC Analysis:

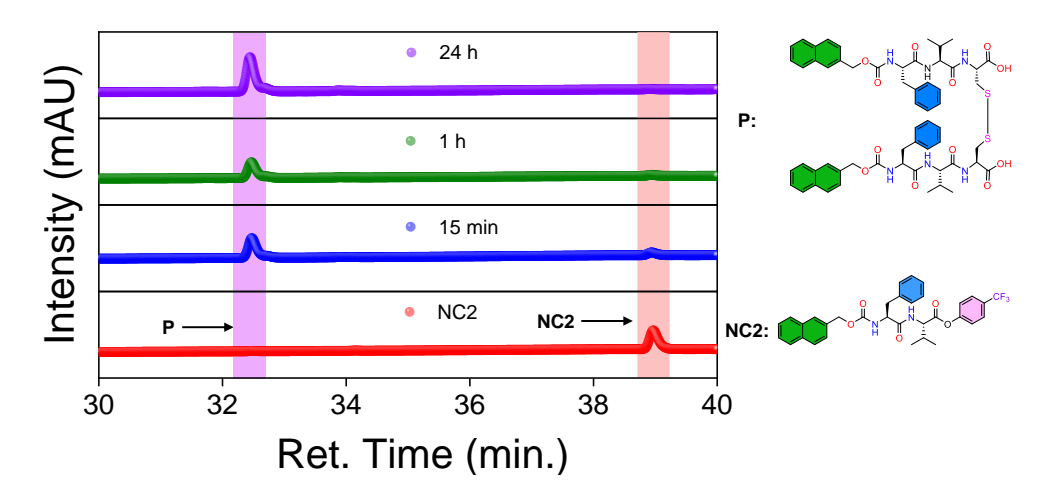


Figure 28. HPLC chromatogram shows the conversion of NC2 with the time

HPLC was used to analysed the NCL product formation. In the chromatogram, **NC2** shows a peak at 39. Then after the initiation of the reaction, chromatogram shows the NCL formation. HPLC analysis shows 99% NCL formation at 24 h (**Figure 28**).

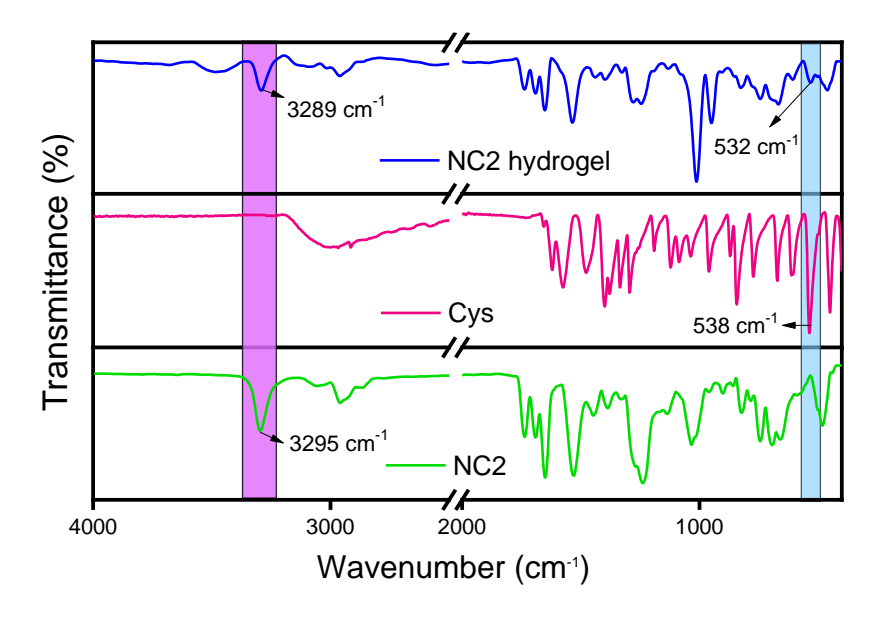


Figure 29. FT-IR spectra of the NC2 hydrogel, Cys and NC2.

The peak at 32.5 appeared due to the NCL formation. As described in native chemical ligation (NCL), an initial $S \to S$ trans-thio esterification is followed by an $S \to N$ acyl shift, ultimately yielding the desired ligated product. In oxoester mediated NCL, the thiol group of cysteine attacks the 4-(trifluoromethyl)phenyl ester, resulting in the formation of a thioester intermediate via an $O \to S$ exchange, which subsequently undergoes an $S \to N$ acyl transfer to generate a native peptide bond. The FT-IR spectra support the formation of NCL. The peak at 532 cm⁻¹ in the FT-IR spectra of NC2 hydrogel represents the stretching of S-S bond (Figure 29). Interestingly, no such peaks are observed in FT-IR spectrum of the NC2. This observation revealed the formation of NCL product.

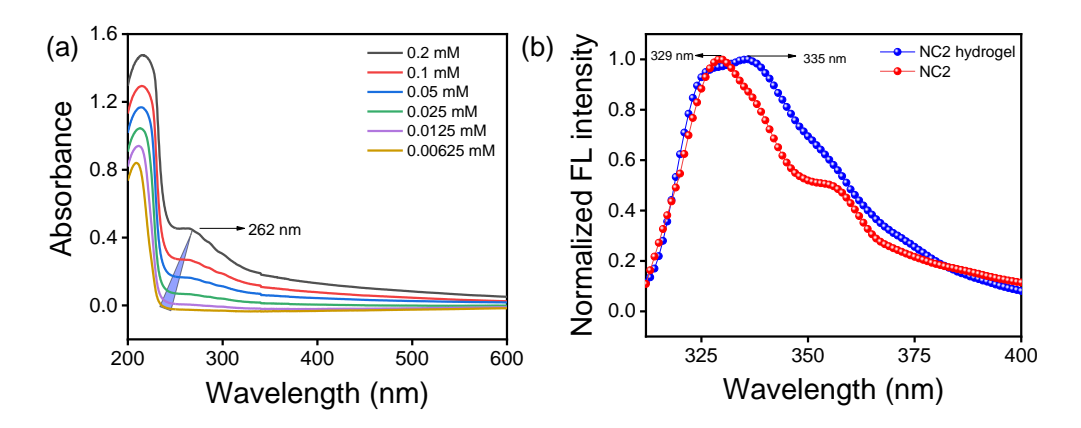


Figure 30. (a) Concentration dependent UV-vis spectra of the NC2 (b) The normalized fluorescence emission spectra of the NC2 and NC2 hydrogel.

UV-Vis and fluorescence spectroscopy were employed to investigate the self-assembly process. UV-vis spectra were obtained for NC2 hydrogel, with absorption peaks observed in the 200–300 nm range. Notably, the UV-Vis spectrum of the NC2 hydrogel exhibited a peak at 262 nm for the higher concentration, suggesting the formation of a higher-order supramolecular assembly within the hydrogel matrix (Figure 30a). Fluorescence spectra were recorded for both the substrate solutions and the NC2 hydrogel. The NC2 solution displayed an emission peak at 335nm. Upon the addition of cysteine in the NC2 which mediate the NCL, as a consequence a red shift in the

emission maximum was observed in NC2 hydrogel, indicating a transition to longer wavelengths (Figure 30b). This spectral shift is attributed to the formation of the hydrogel, reflecting changes in the molecular environment associated with higher-order assembly.

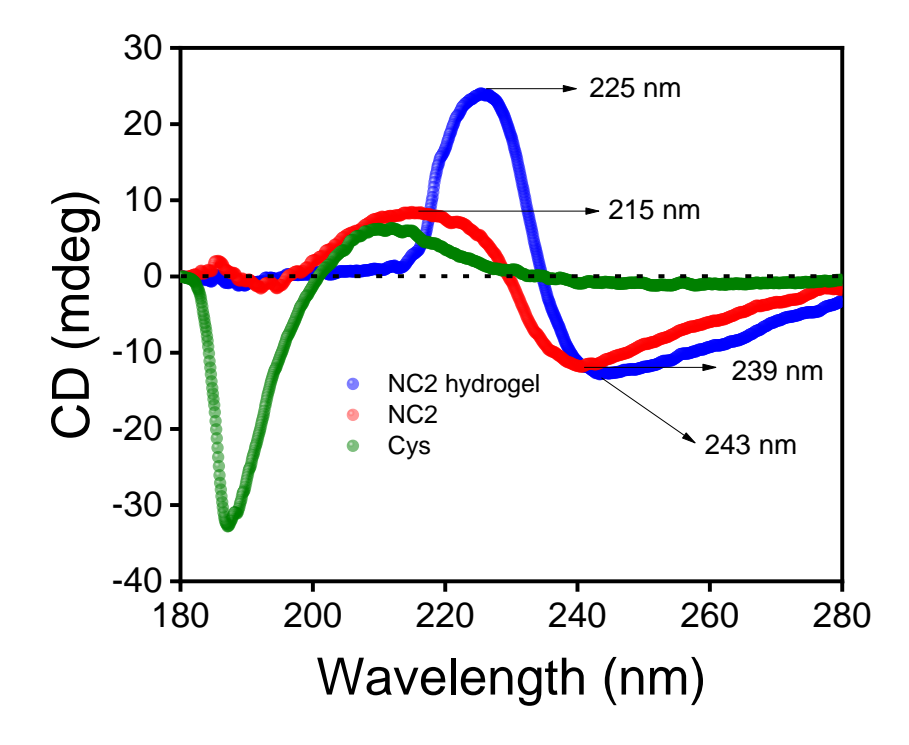


Figure 31. CD spectra of the NC1 hydrogel solution (blue line), NC1 (red line) and Cys (green line).

Circular dichroism spectroscopy serves as an essential analytical tool for assessing the secondary structural features of biomolecules, including proteins and nucleic acids. Circular dichroism (CD) spectroscopy was utilized to analyze the secondary structure of the peptide in the gel phase. The CD spectrum of **Cys** exhibited a negative band at 188 nm, indicative of a rancom coil structure (**Figure 31**). In contrast, the CD spectra of **NC2** and **NC2** hydrogel exhibit features indicative of a twisted or helical conformation. The presence of positive and negative bands at 225 nm and 239 nm in the CD spectrum suggests a twisted conformation of the self-assembled peptides, likely arising from the supramolecular organization of the peptide molecules (**Figure 31**). A significant red shift in the CD spectra of the **NC2** hydrogel

suggests the presence of the higher order self-assembly which helps in the formation of the hydrogel.

Rheological Study:

Rheological measurements were carried out at 25 °C using an Anton Paar Physica MCR 301 Rheometer. To evaluate the viscoelastic behaviour of the hydrogels, the storage modulus (G') and loss modulus (G") were recorded. Freshly prepared hydrogels were carefully placed on the rheometer stage, and a solvent trap was used to prevent dehydration during analysis. A 25 mm diameter parallel plate with a set gap of 0.5 mm was employed for the experiments. The plots in **Figure 32a and 32b** show that the viscous modulus (G") is comparatively lower than the elastic modulus (G'), thereby confirming the gel state of the swelled **NC2**. The increasing nature of both moduli against frequency is also evident from **Fig 32(a)**, which suggests the elastic nature of the **NC2** hydrogel.

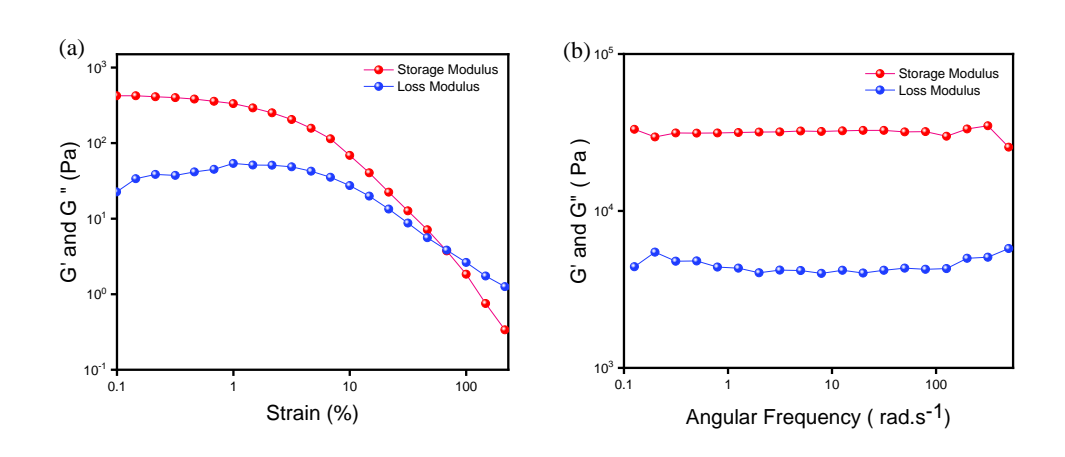


Figure 32. Plots of (a) Storage modulus and Loss modulus vs. Strain (%), (b) Storage modulus and Loss modulus vs. Angular frequency, determined the rheology experiment of **NC1** hydrogel.

CLSM analysis:

The structural morphology of the NC2 hydrogel was examined using advanced microscopic techniques, such as confocal laser scanning microscopy (CLSM). The CLSM image demonstrate the presence of the twisted nanofiber which helps to form the NC2 hydrogel. The average width of the fibre is 80 nm (Figure 33).

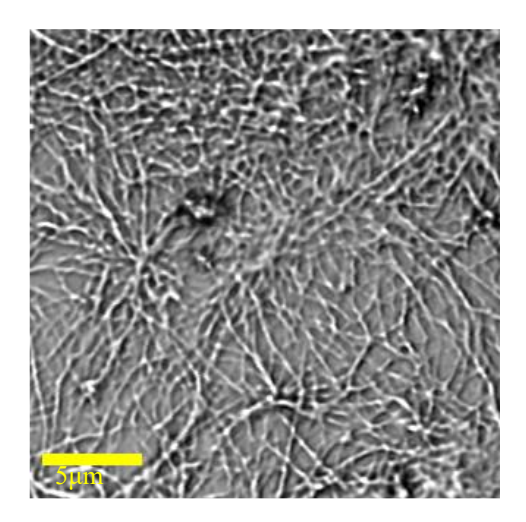


Figure 33. The CLSM images of NC2 hydrogel. The scale bar is 5 μ m. The image was taken using 100x at z1.0 magnification.

CHAPTER - 6

6.1 Conclusion:

This research focused on the development and application of oxo-ester-mediated native chemical ligation (NCL) as a versatile strategy for peptide synthesis and self-assembly. The successful synthesis of novel fluorinated phenyl ester derivatives as acyl donors played a central role in promoting efficient and selective ligation under mild, aqueous conditions. These activated esters demonstrated high reactivity toward N-terminal cysteine-containing peptides, leading to the formation of peptide bonds without the need for external thiol additives, thereby simplifying the reaction conditions and enhancing the biocompatibility of the process.

The resulting peptides underwent spontaneous self-assembly into well-defined supramolecular structures, including hydrogels. These self-assembled materials were extensively characterized using techniques such as nuclear magnetic resonance (NMR), confocal laser scanning microscopy (CLSM), and rheological analysis. The data revealed that the structural organization and viscoelastic behaviour of the hydrogels were significantly influenced by the nature of the fluorinated leaving group, suggesting a direct relationship between ester structure and self-assembly behaviour.

Overall, the findings demonstrate the potential of oxo-ester-mediated NCL as a powerful tool in the design of peptide-based soft materials. The approach provides a chemically robust and modular platform for synthesizing functional biomaterials with applications in tissue engineering, drug delivery, and biomedical diagnostics. By deepening the understanding of peptide self-assembly mechanisms and the role of chemical structure in influencing supramolecular organization, this study contributes meaningfully to the expanding field of peptide-based material science. Future investigations may explore the incorporation of additional functional motifs, stimuli-responsive behaviour, or bioactive sequences to further broaden the applicability of this approach in real-world biomedical contexts.

6.2 Scope of work:

Building on the findings of this study, future research could explore the incorporation of stimuli-responsive functionalities into the peptide scaffolds to create dynamic and adaptive biomaterials. For instance, integrating redox-sensitive, photo-switchable, or pH-responsive groups could enable precise control over self-assembly, disassembly, and cargo release in a biologically relevant environment. Additionally, expanding the current strategy to longer and more complex peptide sequences could facilitate the development of hierarchically organized structures with defined biological functions.

Another promising direction is the integration of bioactive peptide sequences that promote cell adhesion, differentiation, or targeted therapeutic action, thereby enhancing the biomedical applicability of these materials in tissue engineering and drug delivery systems. Investigating in vivo biocompatibility, degradation behaviour, and therapeutic performance of these hydrogels will also be essential for translating this platform to clinical or diagnostic settings.

Overall, the oxo-ester-mediated NCL approach presents a robust and flexible foundation for engineering multifunctional peptide materials, opening new possibilities for innovations at the interface of chemistry, biology, and materials science.

REFERENCES

- P. E. Dawson, T. W. Muir, I. Clark-Lewis and S. B. H. Kent, *Science*, 1994, 266, 776–779.
- 2. W. Muramatsu and H. Yamamoto, Org. Lett., 2022, 24, 7194–7199.
- S. Tsuda, T. Yoshiya, M. Mochizuki and Y. Nishiuchi, *Org. Lett.*, 2015, 17, 1806–1809.
- 4. S. Bondalapati, M. Jbara and A. Brik, *Nat. Chem.*, 2016, **8**, 407–418, and references therein.
- 5. S. S. Kulkarni, J. Sayers, B. Premdjee and R. J. Payne, *Nat. Rev. Chem.*, 2018, **2**, 0122, and references therein.
- 6. Q. Wan and S. J. Danishefsky, *Angew. Chem. Int. Ed.*, 2007, **46**, 9248–9252.
- 7. D. B. Rasale and A. Das, *Chem. Commun.*, 2014, **50**, 10289–10308.
- 8. T. M. Hackeng, J. H. Griffin and P. E. Dawson, *Proc. Natl. Acad. Sci. U. S. A.*, 1999, **96**, 10068–10073.
- 9. X. Fan, Y. Wen, H. Chen, B. Tian and Q. Zhang, *Org. Lett.*, 2024, **26**, 5436–5440.
- 10. E. C. B. Johnson and S. B. H. Kent, *J. Am. Chem. Soc.*, 2006, **128**, 6640–6646.
- 11. D. B. Rasale, I. Maity, M. Konda and A. K. Das, *Chem. Commun.*, 2013, **49**, 4815–4817.
- 12. R. E. Thompson, X. Liu, N. Alonso-Garcia, P. J. B. Pereira, K. A. Jolliffe and R. J. Payne, *J. Am. Chem. Soc.*, 2014, **136**, 8161–8164.
- 13. D. B. Rasale, I. Maity and A. K. Das, *Chem. Commun.*, 2014, **50**, 11397–11399.
- 14. H. Wang, Y. Song, W. Wang, N. Chen, B. Hu, X. Liu, Z. Zhang and Z. Yu, *J. Am. Chem. Soc.*, 2024, **146**, 330–341.
- 15. T. S. Chisholm, D. Clayton, L. J. Dowman, J. Sayers and R. J. Payne, *J. Am. Chem. Soc.*, 2018, **140**, 9020–9024.
- S. Suda, T. Yoshiya, M. Mochizuki and Y. Nishiuchi, *Org. Lett.*, 2015,
 17, 1806–1809.
- 17. N. Ollivier, T. Toupy, R. C. Hartkoorn, R. Desmet, J. M. Monbaliu and O. Melnyk, *Nat. Commun.*, 2018, **9**, 2847.

- 18. D. Mandal, A. Nasrolahi Shirazi and K. Parang, *Org. Biomol. Chem.*, 2014, **12**, 3544–3561.
- 19. N. J. Mitchell, L. R. Malins, X. Liu, R. E. Thompson, B. Chan, L. Radom and R. J. Payne, *J. Am. Chem. Soc.*, 2015, **137**, 14011–14014.
- J. Sayers, P. M. T. Karpati, N. J. Mitchell, A. M. Goldys, S. M. Kwong,
 N. Firth, B. Chan and R. J. Payne, *J. Am. Chem. Soc.*, 2018, **140**, 13327–13334.
- 21. L. R. Malins and R. J. Payne, *Curr. Opin. Chem. Biol.*, 2014, **22**, 70–78, and references therein.
- 22. S. B. H. Kent, *Chem. Soc. Rev.*, 2009, **38**, 338–351, and references therein.
- 23. L. Raibaut, N. Ollivier and O. Melnyk, *Chem. Soc. Rev.*, 2012, **41**, 7001–7015, and references therein.
- 24. R. E. Thompson, B. Chan, L. Radom, K. A. Jolliffe and R. J. Payne, *Angew. Chem. Int. Ed.*, 2013, **52**, 9723–9727.
- 25. D. Bang, B. L. Pentelute and S. B. H. Kent, *Angew. Chem. Int. Ed.*, 2006, **45**, 3985–3988.
- 26. E. E. Watson, X. Liu, R. E. Thompson, J. Ripoll-Rozada, M. Wu, I. Alwis, A. Gori, C.-T. Loh, B. L. Parker and G. Otting, ACS Cent. Sci., 2018, 4, 468–476.
- N. Ollivier, J. Dheur, R. Mhidia, A. Blanpain and O. Melnyk, *Org. Lett.*, 2010, 12, 5238–5241.
- N. Ollivier, J. Vicogne, A. Vallin, H. Drobecq, R. Desmet, O. El Mahdi,
 B. Leclercq, G. Goormachtigh, V. Fafeur and O. Melnyk, *Angew. Chem. Int. Ed.*, 2012, 51, 209–213.
- 29. J. B. Blanco-Canosa and P. E. Dawson, *Angew. Chem. Int. Ed.*, 2008, **47**, 6851–6855.
- 30. G. M. Fang, Y. M. Li, F. Shen, Y. C. Huang, J. B. Li, Y. Lin, H. K. Cui and L. Liu, *Angew. Chem. Int. Ed.*, 2011, **50**, 7645–7649.
- 31. J. S. Zheng, S. Tang, Y. K. Qi, Z. P. Wang and L. Liu, *Nat. Protoc.*, 2013, **8**, 2483–2495.
- 32. D. Bang, N. Chopra and S. B. H. Kent, *J. Am. Chem. Soc.*, 2004, **126**, 1377–1383.